AD

USAAVLABS TECHNICAL REPORT 66-16

DEVELOPMENT OF TECHNIQUES FOR THE STATIC AND DYNAMIC ANALYSIS OF FLUID STATE COMPONENTS AND SYSTEMS

By

C. A. Belsterling

February 1966

U. S. ARMY AVIATION MATERIEL LABORATORIES
FORT EUSTIS, VIRGINIA

CONTRACT DA 44-177-AMC-284(T)
ASTROMECHANICS RESEARCH DIVISION
GIANNINI CONTROLS CORPORATION
MALVERN, PENNSYLVANIA

Disclaimers

The findings in this report are not to be construed as an official Department of the Army psoition unless so designated by other authorized documents.

When Government drawings, specifications, or other data are used for any purpose other than in connection with a definitely related Government procurement operation, the United States Government thereby incurs no responsibility nor any obligation whatsoever; and the fact that the Government may have formulated, furnished, or in any way supplied the said drawings, specifications, or other data is not to be regarded by implication or otherwise as in any manner licensing the holder or any other person or corporation, or conveying any rights or permission, to manufacture, use, or sell any patented invention that may in any way be related thereto.

Trade names cited in this report do not constitute an official endorsement or approval of the use of such commercial hardware or software.

Disposition Instructions

Destroy this report when no longer needed. Do not return it to originator.

DEPARTMENT OF THE ARMY
U. S. ARMY AVIATION MATERIEL LABORATORIES
FORT EUSTIS, VIRGINIA 23604

This report has been reviewed by the U. S. Army Aviation Materiel Laboratories and is considered to be technically sound. The report is published for the exchange of information and the stimulation of ideas.

Task 1P121401A14186
Contract DA-44-177-AMC-284(T)
USAAVLABS Technical Report 66-16
February 1966

DEVELOPMENT OF TECHNIQUES FOR THE STATIC AND DYNAMIC ANALYSIS OF FLUID STATE COMPONENTS AND SYSTEMS

Final Report
Report No. ARD-FR-037

by

C. A. Belsterling

Prepared by

Astromechanics Research Division
Giannini Controls Corporation
Malvern, Pennsylvania

For

U.S. Army Aviation Materiel Laboratories
Fort Eustis, Virginia

ABSTRACT

This report describes development of analytical techniques necessary for design of systems using fluidic components. It covers the analytical and experimental work on five separate tasks intended to extend the usefulness of previously conceived methods. The results lead to the following conclusions:

1) Valid equivalent circuits have been developed to describe the dynamic behavior of most fluid amplifiers.
2) These equivalent circuits are useful for frequencies from zero through 2000 cps.
3) The validity of certain methods previously developed for evaluating equivalent circuit elements has been confirmed.
4) Static characteristic curves of amplifier performance of the type developed under this program can be normalized, thereby minimizing the number of sets of curves necessary to describe the behavior of an amplifier.
5) The mathematical model derived for a simple impedance element is valid for low values of through-flow; additional work is needed to modify it for high through-flow values.

PREFACE

The work covered in this report was conducted by the Astromechanics Research Division of Giannini Controls Corporation at Malvern, Pennsylvania, during the period March 1, 1965 through October 31, 1965. C. A. Belsterling, Chief, Fluid State Systems, was Project Engineer, principal investigator, and author of this report. Dr. P. A. Orner, Staff Scientist, was the major contributor to the work on impedance elements, and N. G. Barr conducted much of the experimental testing.

The project was performed under Contract DA-44-177-AMC-284(T) with the U.S. Army Aviation Materiel Laboratories. George Fosdick was the Government's project monitor. Related reports and technical papers are listed in the Bibliography.

TABLE OF CONTENTS

LIST OF ILLUSTRATIONS

LIST OF SYMBOLS

A	effective cross sectional area (in^2)
B	friction parameter
V/P_{abs}	equivalent capacitance (in^5/lb)
C_c	amplifier control capacitance (in^5/lb)
C_o	amplifier output capacitance (in^5/lb)
C_L	load capacitance (in^5/lb)
C_t	total output circuit capacitance (in^5/lb)
C'	capacitance associated with separation time constant (in^5/lb)
c	isothermal acoustic velocity (in/sec)
e	base of natural logarithms
f	frequency (cycles per second)
G	length factor
j	imaginary factor
K	orifice constants
K_p	amplification factor $\delta P_o / \delta P_{cd}/Q_o$ constant
K_p'	fictitious open-loop amplification factor
L	equivalent inductance $\rho \ell / A$ ($lb.sec^2/in^5$)
L_c	amplifier control inductance ($lb.sec^2/in^5$)
L_o	amplifier output inductance ($lb.sec^2/in^5$)
ℓ	length (in)
M	amplitude ratio
P	pressure (psi)
P_{abs}	mean absolute pressure (psi)

P_c	control pressure (psi)
P_{cd}	control differential pressure (psi)
P_o	output pressure (psi)
P_{od}	output differential pressure (psi)
P_s	supply pressure (psi)
Q	volume flow (ft^3/min)
Q_{CL}	control flow (ft^3/min)
Q_o	output flow (ft^3/min)
Q_s	supply flow (ft^3/min)
R	equivalent resistance $\Delta P/ \Delta Q$ ($lb.sec/in^5$)
R_c	amplifier input (control) resistance ($lb.sec/in^5$)
R_o	amplifier output resistance ($lb.sec/in^5$)
R_L	load resistance ($lb.sec/in^5$)
R'	resistance associated with separation time constant ($lb.sec/in^5$)
s	Laplace transform variable (1/sec)
T	termination factor
t_d	amplifier time delay (sec)
U_o	quiescent through-flow factor
u_o	quiescent through-flow (in/sec)
V	volume (in^3)
Z	effective impedance ($lb.sec/in^5$)
Z_c	impedance of finite tube with zero quiescent flow ($lb.sec/in^5$)
Z_t	termination impedance ($lb.sec/in^5$)

Z_∞	impedance of semi-infinite tube with zero quiescent flow ($lb.sec/in^3$)
Φ	relative phase angle (degrees)
ω	radian frequency (radians/sec)
ρ	mean air density ($lb.sec^2/in^4$)

SUMMARY

This report describes development of analytical techniques necessary for design of control systems using fluidic components. It covers the analytical and experimental work on five separate tasks intended to extend the usefulness of previously conceived and validated methods. The five tasks were:

1) Analysis of three additional amplifier designs, including a vented jet interaction amplifier, a closed jet interaction amplifier, and a vented elbow amplifier.
2) Experimental test and correlation with the analysis of the three additional designs under Task 1.
3) Analysis, test, and correlation of the dynamic response of a vented jet interaction amplifier at frequencies up to 2000 cps.
4) Normalization of the static input and output characteristics of a vented jet interaction amplifier.
5) Analysis, test, and correlation of the dynamic behavior of typical load impedances at frequencies up to 400 cps.

Equivalent circuits representing the three new amplifier designs were developed, and a mathematical model for a simple tubular impedance with quiescent through-flow was derived and experimentally verified.

CONCLUSIONS

The results of the program described in this report, including an evaluation of the correlation between analytical and experimental results, lead to the following conclusions:

1) Valid equivalent circuits have been developed to describe the dynamic behavior of most fluid amplifiers.
2) These equivalent circuits are useful for frequencies from zero through 2000 cps.
3) The validity of the methods previously developed for evaluating equivalent circuit elements has been confirmed.
4) Static characteristic curves of amplifier performance of the type developed under this program can be normalized, thereby minimizing the number of sets of curves necessary to completely describe the behavior of an amplifier.
5) The mathematical model derived for a simple impedance element is valid for low values of through-flow; additional work is needed to modify it for high through-flow values.

RECOMMENDATIONS

This research program has yielded a methodology which provides the control systems designer with the analytical tools for:

1) Defining and specifying the static characteristics of components.
2) Defining and specifying the dynamic characteristics of components.
3) Matching the static characteristics of components in control systems.
4) Integrating and optimizing the dynamic performance of components in control systems.
5) Optimizing the design dimensions of individual components.

The methodology developed constituted progress in two definite directions: first, and of immediate importance, in providing the tools for systems design, and second, as a kind of by-product, in making available the means to optimize components. Therefore, it is recommended that the following tasks be undertaken:

Task A - Prepare a fluidic systems design guide consolidating the results of work to date in a form useful to all control systems engineers.

Task B - Apply the analytical techniques developed under this program in a knowledgeable approach to optimizing the design dimensions of individual fluidic components.

INTRODUCTION

This report describes the progress made in an eight-month project intended to extend the usefulness of previously developed techniques for the analysis and design of fluid state systems. The project was one phase of a continuing program to conceive, validate, and publish a complete methodology for the straightforward (not "cut and try") design of systems using fluidic devices.

The overall objective of the program was to develop the analytical techniques necessary for a knowledgeable approach to the design of V/STOL (and other) control systems using fluidic devices. Since most control engineers are familiar with the "black box" approach, it has been applied in the development of these techniques. The first phase of the program covered the definition of valid static characteristic curves and low-frequency (0-1 cps) equivalent electrical circuits (references 3 and 4). The second phase included the conception and validation of the equivalent circuit for a single amplifier design at intermediate frequencies (0-400 cps) (references 1 and 2). The third phase, covered by this report, was intended to extend the previous work to cover three more amplifier designs and frequencies up to 2000 cps. It included the analysis and experimental testing associated with five separate tasks. Its objective was to prove that these new systems design techniques are applicable to a broad range of circuit and performance situations.

STATEMENT OF THE PROBLEM

GENERAL

The need for valid practical analytical techniques for applying fluidic devices in control systems is a generally established fact (references 5 and 6). Because of the insight it provides and the ease with which it can be handled mathematically, the "black box" approach is the best means for satisfying this need within a reasonable time. Therefore, we are applying this approach by developing both graphical and equivalent circuit representations of fluidic devices and validating them by experiment. In doing so, we make available to the fluidic system designer all of the mathematical tools developed over many years in the fields of electronics and servomechanisms.

To illustrate the approach, Figure 1 shows how the total behavior of most fluidic components can be represented by three sets of characteristics. The input characteristics describe what the applied control signal sees when it is connected to the component. The transfer characteristics define how the output would respond to the applied input signal if it were not loaded. The output characteristics show how the signal is affected by any other device connected to its output ports. Note that for the static and large signal cases the characteristics are described graphically; for the dynamic and small signal cases they are described as equivalent electrical circuits.

When fluidic components are described in terms of their input, transfer, and output characteristics, system integration can proceed in an orderly manner. For example, suppose it is necessary to amplify the signal from a rate sensor as illustrated in Figure 2. In this case the output characteristics of the rate sensor, defining the effect of loading, must be matched with the input characteristics of the amplifier, describing how a signal is affected when applied to the input ports. Thus the amplifier input becomes the load on the rate sensor output. (Note that in many practical situations, the static input characteristics are described by a single curve.)

Because the amplifier input circuit becomes the load on the rate sensor, the static performance of the coupled components can be determined by superimposing the amplifier input curve on the family of rate sensor output characteristics. Now, since the coupled circuits are forced to have the same pressures and flows, the only possible operating points are at the intersections of the curves. Therefore, the behavior of the coupled circuits can be plotted from the values of rate input and the amplifier input pressure.

To carry the analysis to completion, we must also consider the fact that

the amplifier, too, will be loaded by some finite impedance. The characteristics of this impedance are then plotted on the output characteristics of the amplifier to define the behavior of the loaded amplifier in response to input pressure signals. Combining this performance with the performance of the loaded rate sensor described in the preceding paragraph results in a single curve defining the output pressure (or flow) from the amplifier in response to rate inputs.

The same process can be followed to define the incremental dynamic response, using equivalent electrical circuits as shown in Figure 3. Here the output circuit of the rate sensor becomes coupled with the input circuit of the amplifier. By solving the equations for each coupled circuit, then combining the three, it is a relatively simple matter to derive the dynamic transfer function for output pressure in response to rate of turn.

DESCRIPTION OF OBJECTIVES

In two previous phases of the program described in this report, static characteristics and dynamic equivalent circuits had been conceived and validated for a single amplifier (HDL 933) at frequencies up to 400 cps. In this phase of the program, the approach was extended to embrace the following additional items:

Task 1	Analysis of three additional amplifier designs, including a vented jet interaction amplifier, a closed jet interaction amplifier, and a vented elbow amplifier.
Task 2	Experimental test and correlation with the analysis of the three additional designs of Task 1.
Task 3	Analysis, test, and correlation of the dynamic response of a vented jet interaction amplifier at frequencies up to 2000 cps.
Task 4	Normalization of the static input and output characteristics of a vented jet interaction amplifier.
Task 5	Analysis, test, and correlation of the dynamic behavior of typical load impedances at frequencies up to 400 cps.

TASK ACCOMPLISHMENTS

TASK 1

Description of Test Amplifiers

Task 1 was intended to develop the equivalent electric circuits representing the dynamic behavior of three amplifier designs up to 400 cps. The three designs chosen for analysis and test were a vented jet interaction amplifier with the dimensions shown in Figure 4, a closed jet interaction amplifier with the dimensions shown in Figure 5, and a vented elbow amplifier with the dimensions shown in Figure 6. The first design is a standard proportional amplifier (Model 1602) (shown in Figure 7) purchased from Corning Glass. The second is the HDL 933 design with closed vents (Figure 8) fabricated in PLEXIGLAS on our pantograph milling machine. The third is a scaled-down double leg elbow amplifier (Figure 9) also fabricated in PLEXIGLAS on our pantograph milling machine.

Analysis of the Amplifier Dynamics

Dynamic analysis were carried out on each of the three amplifier configurations considering frequencies up to 400 cps. The results were applied to define the equivalent electrical circuits which would behave in a manner analogous to the fluidic device. Figure 10 shows the equivalent circuit for the vented jet interaction amplifier. It is identical to the circuit previously developed for the vented HDL 933 design. The transfer function is shown in Figure 10.

Figure 11 shows the equivalent circuit for the closed jet interaction amplifier. It is similar to the circuit for the vented amplifier except that the values of the circuit elements are considerably different and there is an internal feedback path of load pressure delayed by the charging time of the output circuit. The transfer function is shown in Figure 11.

The equivalent circuit for the vented elbow amplifier is shown in Figure 12. It differs from the vented jet interaction amplifier in the addition of an isolated RC circuit representing the time constant associated with the dynamics of the separation point. The transfer function is shown in Figure 12.

TASK 2

Construction of Signal Generator

The objective of Task 2 was to test and correlate the experimental frequency response of the three amplifiers of Task 1 up to a frequency

of 400 cps. Before this could be done, it was necessary to design and fabricate a sinusoidal pressure signal generator to provide the input test signal. Mechanical parts for the signal generator were fabricated in the experimental shop. An electronic speed controller and drive motor were purchased. Figure 13 contains photographs of the hardware. At the upper right is the main assembly, including a cylindrical housing supported on three legs and a vertically mounted universal motor with shaft and hub protruding into the housing. Front and center of 13(a) are the two signal generating discs, one of which is shaped and mounted on the hub as shown in Figure 13(b). At the left of the motor-housing assembly is the electronic speed control unit, which permits continuous variation of the motor speed from zero to 12,000 rpm.

The signal generator is essentially a motor-driven wobble plate with two impinging nozzles which form the active legs of a pneumatic Wheatstone bridge circuit. With a supply pressure to the bridge as shown in Figure 14, a differential pressure signal which is very nearly sinusoidal is generated at the adjacent terminals of the bridge. Two disc shapes are used to cover the range of frequencies required by the present project. Typical signals generated by the discs are shown in Figure 15.

Test of Vented Jet Interaction Amplifier

Frequency response tests were run on the vented jet interaction amplifier (Corning Model 1602-A) with minimum-volume circuits. The test circuit is shown schematically in Figure 16. Typical data recorded on the oscilloscope are shown in Figure 17. The results are plotted in Figure 18.

Static characteristics were also recorded for the vented amplifier using the variable-load test method. The output characteristics are shown in Figure 19, and the input characteristics are shown in Figure 20.

Test of Closed Jet Interaction Amplifier

Frequency response tests were run on the closed jet interaction amplifier with minimum-volume circuits. The test circuit was identical with the one shown in Figure 16. Test results are plotted in Figure 21.

Static characteristics were also recorded for the closed amplifier using the variable-load test method. The output characteristics are shown in Figure 22, and the input characteristics are shown in Figure 23.

Test of Vented Elbow Amplifier

Frequency response tests were run on the vented double leg elbow amplifier with minimum-volume circuits. The test circuit is shown in Figure 24. Note that the amplifier is operated single-ended and the

unused outlet port is vented to atmosphere. Test results are plotted in Figure 25.

Static characteristics were also recorded for the elbow amplifier using the variable-load test method. The output characteristics are shown in Figure 26, and the input characteristics are shown in Figure 27.

TASK 3

Analysis of Beam Dynamics

Task 3 was intended to define the dynamic characteristics of the vented jet interaction amplifier at frequencies up to 2000 cps.

In analyzing the dynamics, it was decided that the equivalent circuit for frequencies up to 400 cps (shown in Figure 10) should hold if the jet beam deflection could still be treated as a simple time delay. This was questionable because of the possibility of increased mixing due to the high shear interfaces and viscous effects in the rapidly undulating jet beam. Therefore, a simple experiment was carried out to establish whether the beam deflection could be treated as a simple time delay at the frequencies of interest.

The experimental apparatus is shown in Figure 28. It consists of a simple tubular power nozzle forming a jet controlled by two tubular control nozzles. Two hot wire anemometers are located in line with the resulting jet, spaced a known distance apart. The signals from these hot wire probes are compared on an oscilloscpe. Phase difference is of primary interest in proving that the beam dynamics can be represented by a simple time delay.

The results of tests using this experimental rig are shown in Figure 29.

Frequency Response Tests

To minimize the effect of circuit elements and concentrate on the high frequency behavior of the amplifier alone, flow response tests were planned originally. Hot wires were inserted directly into the input and output apertures of the Corning Model 1602 amplifier. Signals from these wires were compared on an oscilloscope for relative phase and amplitude. Test results are plotted in Figure 30. Assuming that beam deflection can be treated as a simple time delay, the transfer function at these frequencies is very nearly the time delay alone.

In the process of recording the flow response using hot wires, there was a great deal of difficulty in achieving a reasonable signal-to-noise ratio. Therefore, for backup information, a second model 1602 amplifier was instrumented with miniature pressure transducers, flush-

mounted in the input and output apertures. The signal-to-noise ratio was better in this case and pressure response tests were recorded. Test results are plotted in Figure 31.

Assuming that beam deflection can be treated as a simple time delay, the transfer function for pressure response at these frequencies is derived as

$$P_{od}/P_{cd} = \frac{2K_p R_L}{R_o+R_L} \frac{e^{-st_d}}{\left(1 + s\frac{L_c}{R_c} + s^2 L_c R_c\right)\left[1+s\left(\frac{C_t 2R_o R_L + L_o}{R_o + R_L}\right) + s^2 \frac{2C_t L_o R_L}{R_o + R_L}\right.} \quad (1)$$

where

P_{od} is the output differential pressure (psi)

P_{cd} is the control differential pressure (psi)

K_p is the amplification factor

R_L is the load resistance (lb.sec/in^5)

R_o is the amplifier output resistance (lb.sec/in^5)

e is the base of natural logarithms

s is the Laplace transform variable (1/sec)

t_d is the amplifier time delay (sec)

L_c is the amplifier control inductance (lb.sec^2/in^5)

R_c is the amplifier input resistance (lb.sec/in^5)

C_c is the amplifier input capacitance (in^5/lb.)

C_t is the total output circuit capacitance (in^5/lb.)

R_o is the amplifier output resistance (lb.sec/in^5)

L_o is the amplifier output inductance (lb.sec^2/in^5)

Note that the values of the circuit elements are quite different from the normal case because the transducers are located inside the amplifier. Because of this, the time response is again mainly dependent on the time delay, t_d.

TASK 4

Task 4 was intended to determine whether static characteristic curves of the type generated in this work could be normalized. The object was to minimize the number of sets of curves necessary to describe the characteristics of an amplifier in most circuit connections.

Again the Corning Model 1602-A vented jet interaction amplifier was chosen as the test object. Data were recorded for supply pressures of 2, 4, 6, and 8 psig maintaining control bias at 10% of the supply pressure. The output characteristics were then normalized with respect to supply pressure and supply flow. The results are plotted in Figures 32, 33, 34, and 35.

The input characteristics were first normalized with respect to supply pressure and supply flow, but correlation was poor. This was due to the fact that the relationship between supply pressure and supply flow $Q_s = K_1\sqrt{P_s}$; that is, it behaves like an orifice. On the other hand, the control nozzle behaves more like a laminar restrictor and $Q_c = K_2 P_c$. Therefore, the input curves cannot be normalized with respect to supply flow. The input characteristics were then normalized for supply pressure and square root of supply flow. The results are plotted in Figures 36, 37, 38, and 39.

TASK 5

Analysis of Impedance Elements

Task 5 covered the development of valid mathematical models for simple impedance elements. In this work we considered four cases of increasing complexity, leading to the case with finite through-flow and zero termination impedance. This represents the situation encountered in amplifier circuits when the loads on the output legs are returned to atmosphere. The results of the analytical study are summarized below:

Case I - Semi-infinite, constant area tube with zero quiescent flow.

$$Z_\infty = \frac{c}{A}\sqrt{\frac{j\omega + B}{j\omega}} \qquad (2)$$

where c is the isothermal acoustic velocity (in/sec)

A is the area of tube (in^2)

ω is the radian frequency (radians/sec)

B is the friction parameter

At high frequencies

$$Z_\infty \rightarrow \frac{c}{A} \quad \text{(characteristic impedance)} \tag{3}$$

Case II - Finite length tube with lossless outlet and zero quiescent flow.

$$Z_\ell = Z_\infty \tanh \frac{\ell}{c} \sqrt{j\omega\,(j\omega + B)} \tag{4}$$

or

$$Z_\ell = Z_\infty\, G \tag{5}$$

where ℓ is the length of tube (in)

G is the $\tanh \frac{\ell}{c} \sqrt{j\omega\,(j\omega + B)}$ = length factor

at low frequencies

$$Z_\ell \longrightarrow \frac{\ell}{A} \quad (j\omega + B) \tag{6}$$

Case III - Finite length tube with termination impedance and zero quiescent flow.

$$Z_\ell = Z_\infty\, L\, \frac{1 + Z_t/Z_\infty\, G}{1 + GZ_t/Z_\infty} \tag{7}$$

or

$$Z_\ell = Z_\infty\, GT \tag{8}$$

where Z_t is the termination impedance

T is $\dfrac{1 + Z_t/Z_\infty\, G}{1 + GZ_t/Z_\infty}$ = termination factor

Case IV - Finite length tube with zero termination impedance ($Z_t = 0$) and finite through-flow.

$$Z_\ell = Z_\infty L\, \frac{1}{1 + u_o\, G/AZ_\infty} \tag{9}$$

or

$$Z_\ell = Z_\infty GU_o \tag{10}$$

where u_o is the through-flow (in/sec)

U_o is the through-flow factor $\dfrac{1}{1 + u_o\, G/AZ_\infty}$

At low frequencies

$$Z_{\ell} = \frac{\ell}{A} (j\omega + B) \qquad (11)$$

Since the only variables in equation (11) are ω and U_o, it can be simplified to

$$Z_{\ell} = D \frac{1 + j\omega E}{G + j\omega u_o F}$$

where D, E, and F are constants.

Thus, for a given frequency ω and zero through-flow u_o, the impedance is $D(1 + j\omega E)$ or its equivalent $\ell/A (j\omega + B)$. As the through-flow u_o is increased, the impedance should decrease slowly at low frequencies and more rapidly at the higher frequencies. At high levels of through-flow, the rate of decrease in impedance becomes less because u_o is in the denominator of equation (12). The curve should approach the asymptote $Z_{\ell} = 0$.

For given through-flow u_o, the impedance Z_{ℓ} may increase or decrease with frequency depending on the relative magnitude of E and $u_o F$.

Test of Typical Impedance Element

To test the validity of the mathematical model, experimental tests were conducted on a 3-inch-long, 0.052-inch-inside-diameter tube. The tests results are plotted in Figure 40.

CORRELATION BETWEEN THEORY AND EXPERIMENT

DYNAMIC ANALYSIS TO 400 CPS

Vented Jet Interaction Amplifier

The frequency response of the vented jet interaction amplifier (Corning Model 1602-A, Figure 4) was calculated from the transfer function derived from the equivalent circuit of Figure 10. The constants are defined according to references 2 and 3.

Substituting values of frequency for $s = j2\pi f$ and solving for the relative gain and phase shift yields the results shown in Figure 41 superimposed on the experimental test results (Figure 18). The correlation is good.

Closed Jet Interaction Amplifier

The frequency response of the closed jet interaction amplifier (Figure 5) was calculated using the transfer function derived from the equivalent circuit of Figure 11. The constants are evaluated according to references 2 and 3.

Solving the transfer function for a range of frequencies yields the results shown in Figure 42 superimposed on the experimental plot (Figure 21). Note that there is very good correlation between calculated and experimental results. Especially significant is the fact that the calculated amplitude curve does peak as the experimental curve; this is directly a function of the predicted internal feedback loop.

Vented Elbow Amplifier

The frequency response of the vented elbow amplifier (Figure 6) was calculated using the transfer function derived from the equivalent circuit of Figure 12 neglecting the terms R' and C'. The constants are evaluated according to references 2 and 3.

Solving this transfer function for the range of frequencies of interest yields the results shown in Figure 43 superimposed on the experimental plot (Figure 25). Note that the correlation is good and that the amplitude bandwidth is exceptionally high because the output impedance is much lower than that of the jet interaction amplifier.

DYNAMIC ANALYSIS TO 2000 CPS

Flow Response

Frequency response of the flow response test rig was calculated from the

equivalent circuit of Figure 10. The constants are evaluated according to references 2 and 3.

Solving for the response over the range of frequencies of interest yields the results shown in Figure 44 superimposed on the experimental plot (Figure 30). Note that the phase shift is mainly due to the time delay (transport lag) and that it corresponds quite well with the calculated value of 3.2×10^{-4} seconds. Amplitude correlation is good to 1000 cps.

Pressure Response

Frequency response using the pressure test rig was calculated from the equivalent circuit of Figure 10. The constants are evaluated according to references 2 and 3.

Solving for the response over the range of frequencies of interest yields the results shown in Figure 45 superimposed on the experimental plot (Figure 31). The correlation is not good. Note that the phase shift is actually less than that recorded for the flow response test, an unrealistic behavior which is due to more lag in input pressure sensing than occurs in output pressure sensing.

NORMALIZATION OF STATIC CHARACTERISTICS

Output Characteristics

The normalized output characteristics are shown in Figures 32, 33, 34, and 35 for a wide range of supply pressures. Comparing these figures shows that the curves are coincident within approximately $\pm$ 5%. Considering the wide range of supply pressures and the errors in reading low pressures and flows, this correlation is considered adequate.

Input Characteristics

The normalized input characteristics are shown in Figures 36, 37, 38, and 39. Comparing these figures shows that the curves are coincident within approximately $\pm$ 2% over a wide range of supply pressures and flows.

DYNAMIC ANALYSIS OF IMPEDANCE ELEMENTS

According to the analysis, the behavior of a simple capillary impedance element should conform to the equation

$$Z_{\ell} = D \frac{i + j\omega E}{G + j\omega u_o F} \qquad (13)$$

where

ω is the radian frequency (radians/sec)

u_o is the through-flow velocity (in/sec)

G $\tanh \frac{\ell}{c} \sqrt{j\omega\,(j\omega + B)}$ = (length factor)

ℓ is the length (in)

c is the isothermal acoustic velocity (in/sec)

B is the friction parameter

D, E, and F are constants

Comparing, in a qualitative manner, the experimental results plotted in Figure 40 with the behavior predicted by the above equation, the following is noted:

First, the through-flow u_o has a very definite effect on the impedance Z_ℓ at all frequencies, as predicted. Second, the value of impedance Z_ℓ at zero through-flow u_o agrees with the calculated value (the points marked x in Figure 40) reasonably well. Third, as through-flow u_o is increased from zero, the impedance Z_ℓ decreases for 3 of the 4 frequencies recorded and the rate of decrease is greater for the higher frequencies; all are trends predicted by the above equation. Fourth, the slope of the impedance versus through-flow curves decreases with increasing through-flow, again as predicted.

Fifth, the experimental impedance Z_ℓ passes through a minimum, then increases for higher through-flows, a trend <u>not</u> accounted for by the mathematical model. Sixth, for low values of through-flow u_o, the impedance Z_ℓ increases with frequency as predicted. Seventh, for intermediate values of through-flow u_o, the increase with frequency is less, as predicted. Finally, for high values of through-flow u_o, the increase with frequency becomes very large again, a fact not accounted for in the mathematical model.

From this analysis we can see that correlation at low values of through-flow is good; at high values of through-flow it is poor.

EVALUATION

DYNAMIC ANALYSIS TO 400 CPS

Vented Jet Interaction Amplifier

The remarkably good correlation between calculated and experimental results (Figure 41) leads to the conclusion that the equivalent circuit developed for the vented jet interaction amplifier (Figure 10) is a valid one. It also reinforces the validity of the methods for evaluating the equivalent circuit elements as described in references 2 and 3.

Closed Jet Interaction Amplifier

The excellent correlation between calculated and experimental results (Figure 42) leads to the conclusion that the equivalent circuit developed for the closed jet interaction amplifier (Figure 11) is a valid one. Especially significant is the fact that the notoriously difficult-to-describe internal feedback can be handled in such a simple manner.

Vented Elbow Amplifier

The good correlation between calculated and experimental results (Figure 43) leads to the conclusion that the equivalent circuit developed for the vented elbow amplifier (Figure 12) is a valid one. Since the time constant due to the dynamics involved in the change in separation point (R'C') was neglected in the calculation, it also verifies that this time constant (which is difficult to evaluate) is usually negligible.

DYNAMIC ANALYSIS TO 2000 CPS

Flow Response

The good correlation between calculated phase and experimental phase as shown in Figure 44 leads to the conclusion that the dynamics of jet beam deflection are, in fact, a simple time delay, up to 2000 cps. In addition, it reinforces the validity of the equivalent circuit of Figure 10 and the methods of evaluating circuit elements as described in references 2 and 3. We have not considered the amplitude response correlation because the waveform distortion made it difficult to get reliable readings above 1000 cps.

Pressure Response

The marginal correlation between calculated and experimental pressure

response as shown in Figure 45 led to a reevaluation of the amplifier equivalent circuit. In reviewing the calculation we find that important estimates had to be made in evaluating the equivalent circuit elements of Figure 10. For example, because the output pressure transducer was located inside the amplifier output aperture, it was necessary to estimate how much of the output resistance, capacitance, and inductance came before the pressure transducer and how much came after. Estimates like this are critical to the accuracy of the derived transfer function and, it is believed, are the cause of the marginal correlation. However, since the flow response tests above did, after all, yield data with a high degree of confidence, the marginal results of the pressure response tests are not important to the success of this program.

NORMALIZATION OF STATIC CHARACTERISTICS

Output Characteristics

The good correlation obtained in normalizing the output characteristics (as illustrated by Figures 32, 33, 34, and 35) leads to the conclusion that normalization is, indeed, a valuable means for minimizing the number of sets of curves necessary to completely describe the behavior of a fluidic amplifier. It also confirms that the pressure should be normalized with respect to supply pressure and the flow normalized with respect to supply flow.

Input Characteristics

The excellent correlation obtained in normalizing the input characteristics (as illustrated by Figures 36, 37, 38, and 39) leads to the conclusion that normalization is, indeed, a valuable means for minimizing the number of sets of curves necessary to completely describe the behavior of a fluidic amplifier. It also confirms that the pressure should be normalized with respect to supply pressure and the flow normalized with respect to the supply pressure or the square root of supply flow. Because the flow axis is normalized with respect to a different quantity (square root of supply flow) than are the output characteristics (supply flow), one must be careful in using the normalized input characteristics in the design of cascaded stages. The input characteristics must be converted before superposition as a load line on the output characteristics of the previous stage.

DYNAMIC ANALYSIS OF IMPEDANCE ELEMENTS

With reference to the test results in Figure 40 and the foregoing analysis of correlation with the mathematical model, it is concluded that the model is reasonably valid for low values of through-flow. For the purposes of this phase of the program, it is sufficient. However, it is recommended that additional effort be devoted to defining a mathe-

matical model which will also show good correlation at high through-flows. We also recommend that this type of analysis be extended to cover a number of other impedance elements commonly used in fluidic circuits.

BIBLIOGRAPHY

1) Belsterling, C. A., and Tsui, K. C., "Analysis of the Dynamics of Proportional Pure Fluid Amplifiers", The Franklin Institute Report No. I-B2148-01, under contract no. DA-49-186-AMC-95(D) with Harry Diamond Laboratories, Army Materiel Command, August 1964.

2) Belsterling, C.A., and Tsui, K.C., "Analyzing Proportional Fluid Amplifier Circuits", Control Engineering, Volume 12, no. 8, August 1965, pp. 87-92.

3) Belsterling, C. A., and Tsui, K. C., "Application Techniques for Proportional Pure Fluid Amplifiers", Proceedings of the Fluid Amplification Symposium May 1964, Harry Diamond Laboratories, Volume 1, pp. 163-189.

4) Belsterling, C. A., and Tsui, K. C., "Research on the Performance of Pure Fluid Amplifiers", The Franklin Institute Report No. I-09761-1, August 1963.

5) Brown, F.T., "On the Future of Dynamic Analysis of Fluid Systems", Proceedings of the Fluid Amplification Symposium October 1965, Harry Diamond Laboratories, Volume 1, pp. 251-265.

6) Kompass, E.J., "Perspective on Fluid Amplifiers", Control Engineering, Volume 11, no. 9, September 1964, p. 73.

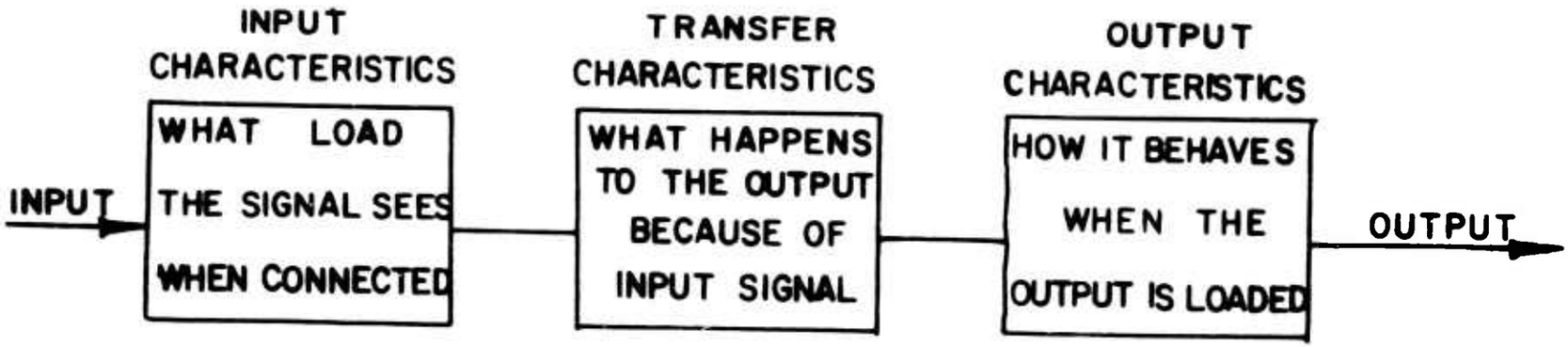

NOTES: 1) FOR STATIC AND LARGE SIGNAL ANALYSIS THESE CHARACTERISTICS ARE EXPRESSED GRAPHICALLY.

2) FOR DYNAMIC AND SMALL SIGNAL ANALYSIS THESE CHARACTERISTICS MAY BE EXPRESSED AS EQUIVALENT ELECTRICAL CIRCUITS.

FIGURE 1- DESCRIPTION OF THE BEHAVIOR OF A FLUIDIC AMPLIFIER.

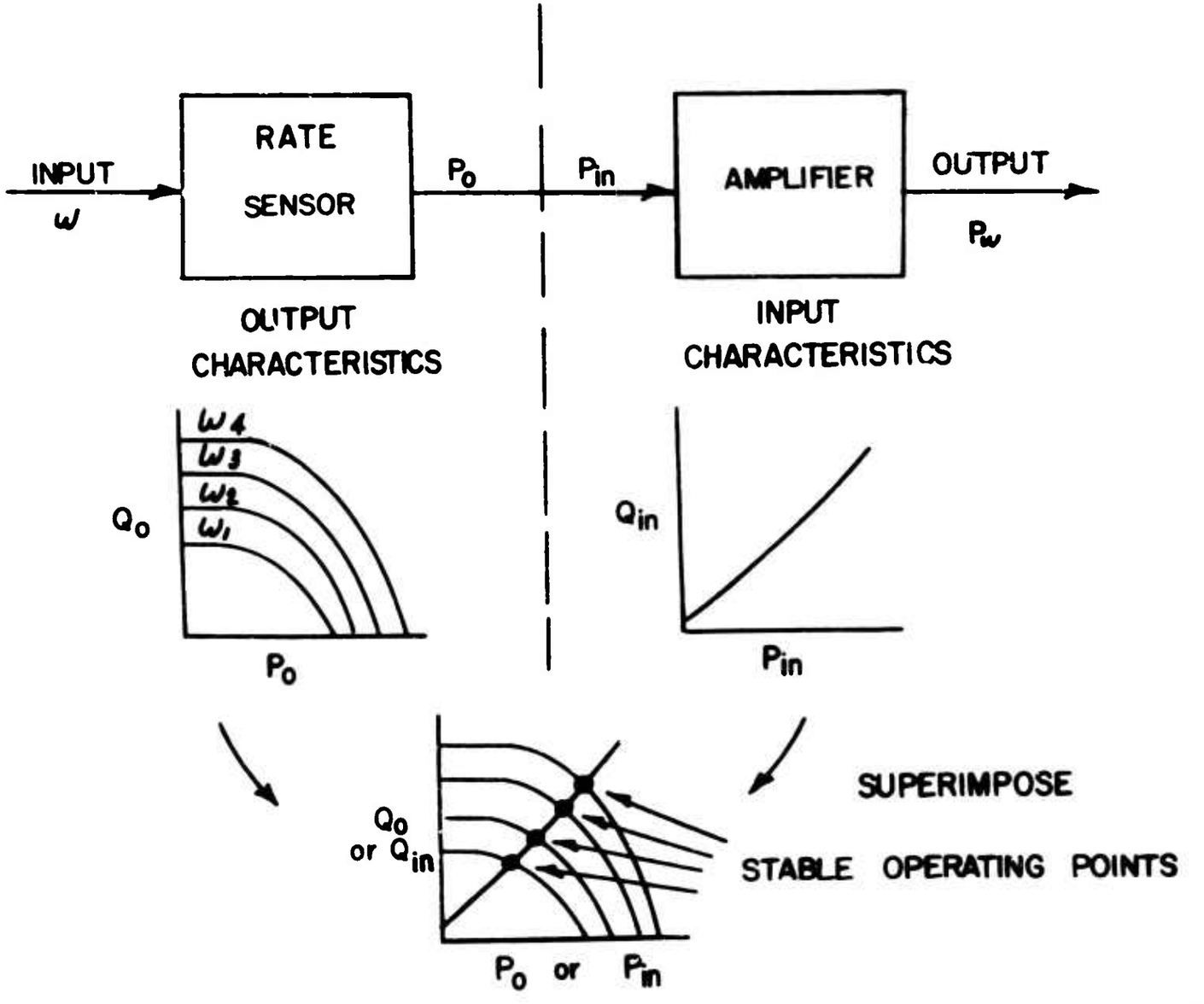

FIGURE 2 - MATCHING STATIC CHARACTERISTICS OF TWO CASCADED COMPONENTS

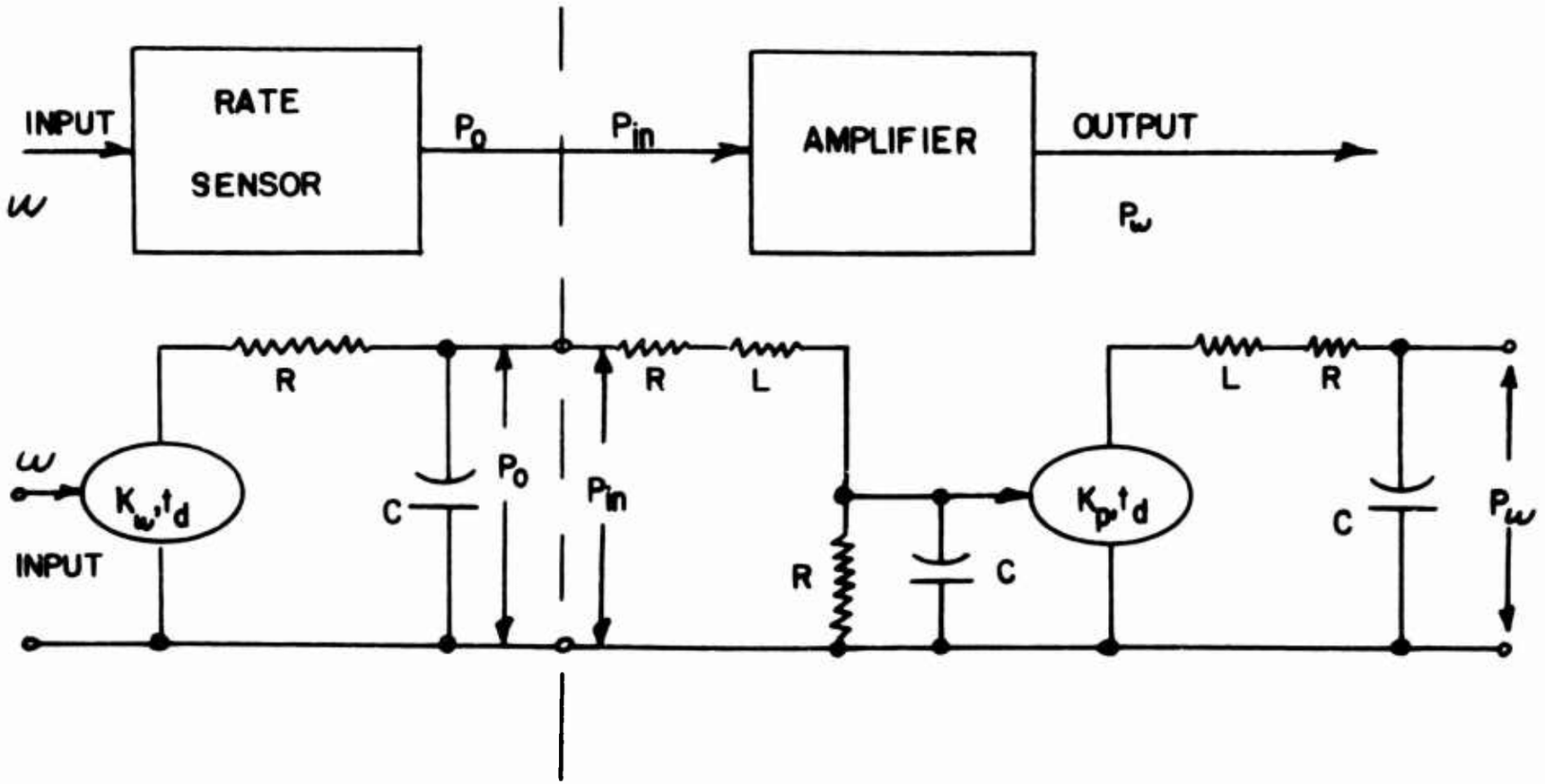

FIGURE 3 - INTEGRATING THE DYNAMIC CHARACTERISTICS OF TWO CASCADED COMPONENTS.

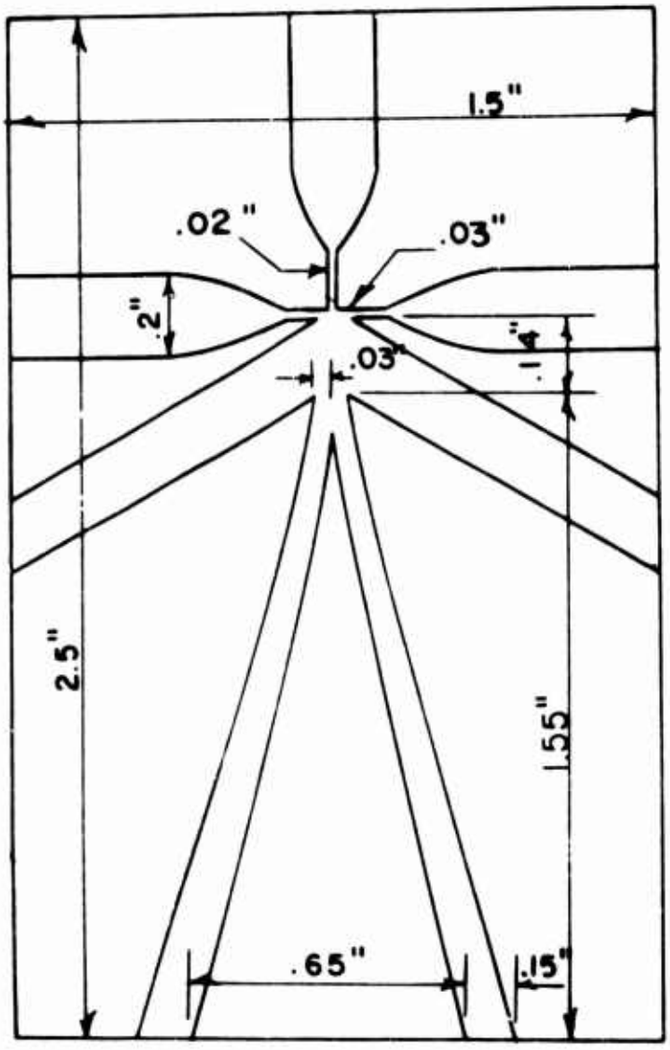

FIGURE 4 – DIMENSIONAL SKETCH OF VENTED JET INTERACTION AMPLIFIER (CORNING MODEL 1602)

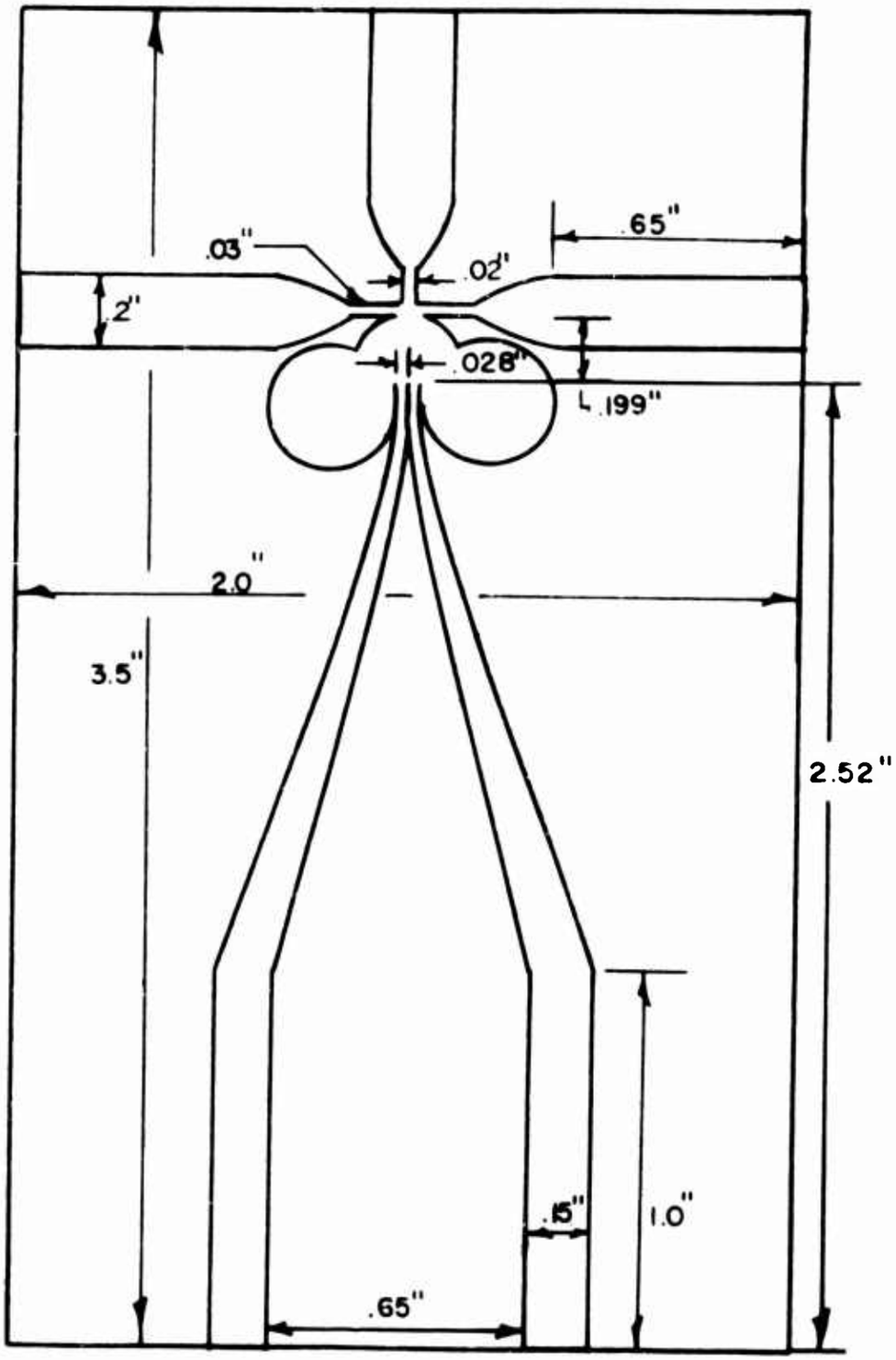

FIGURE 5 - DIMENSIONAL SKETCH OF CLOSED JET INTERACTION AMPLIFIER.

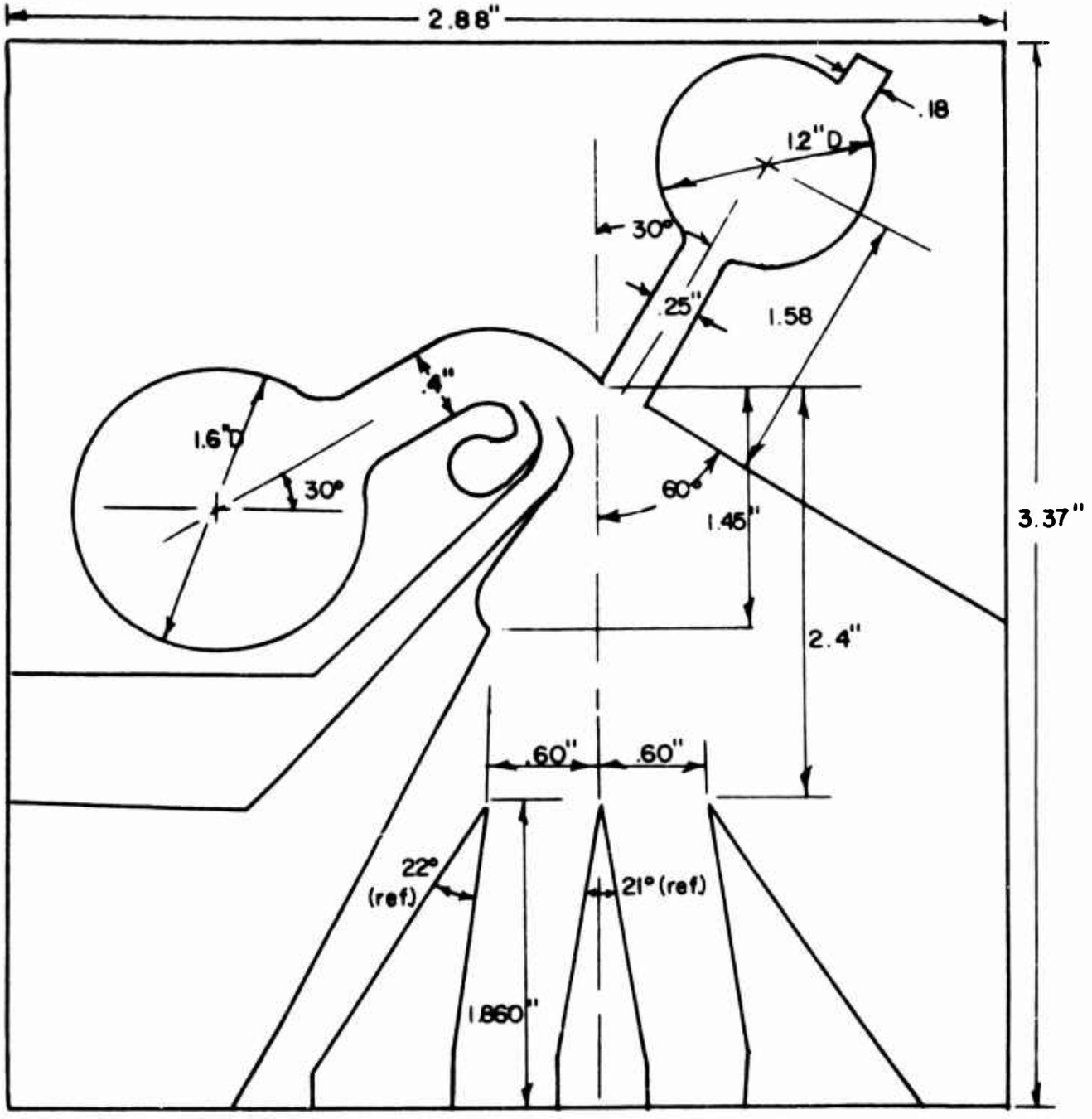

FIGURE 6 - DOUBLE-SIZE DIMENSIONAL DRAWING OF VENTED ELBOW AMPLIFIER.

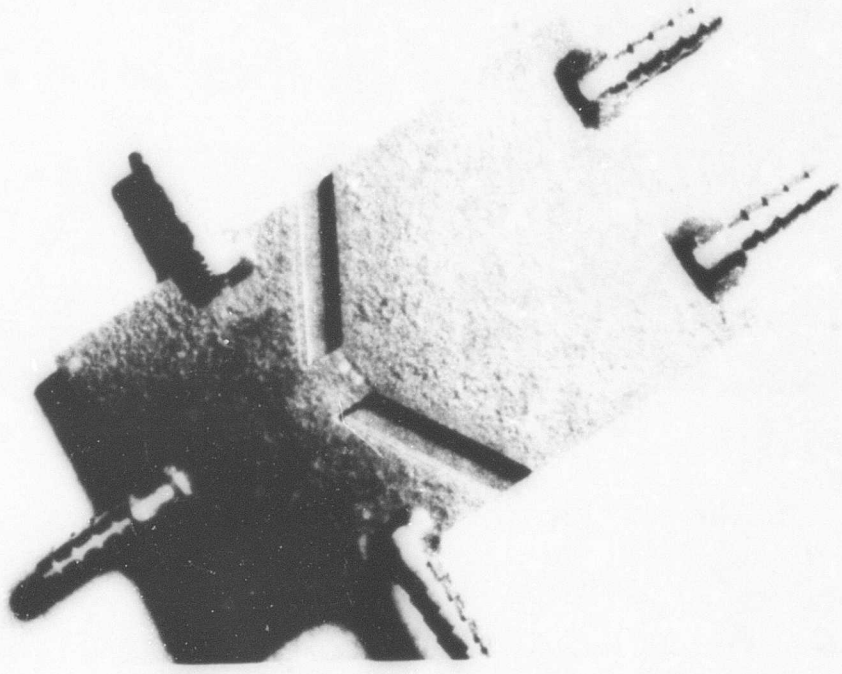

FIGURE 7 - PHOTO OF VENTED JET INTERACTION AMPLIFIER (CORNING MODEL 1602).

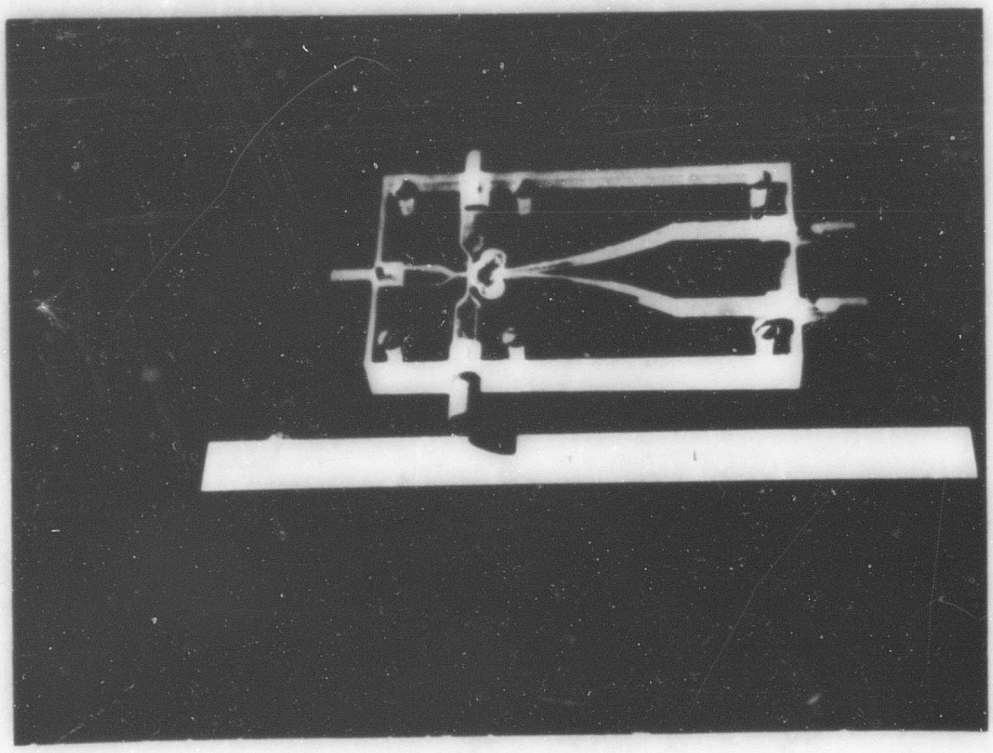

FIGURE 8 - PHOTO OF CLOSED JET INTERACTION AMPLIFIER.

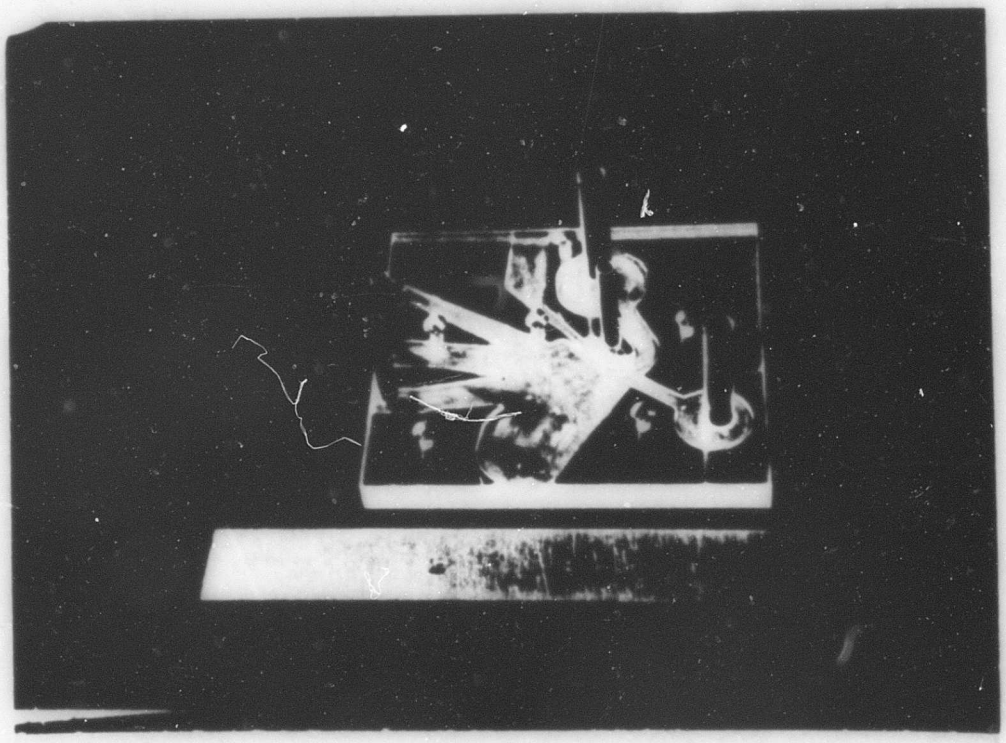

FIGURE 9 - PHOTO OF VENTED ELBOW AMPLIFIER.

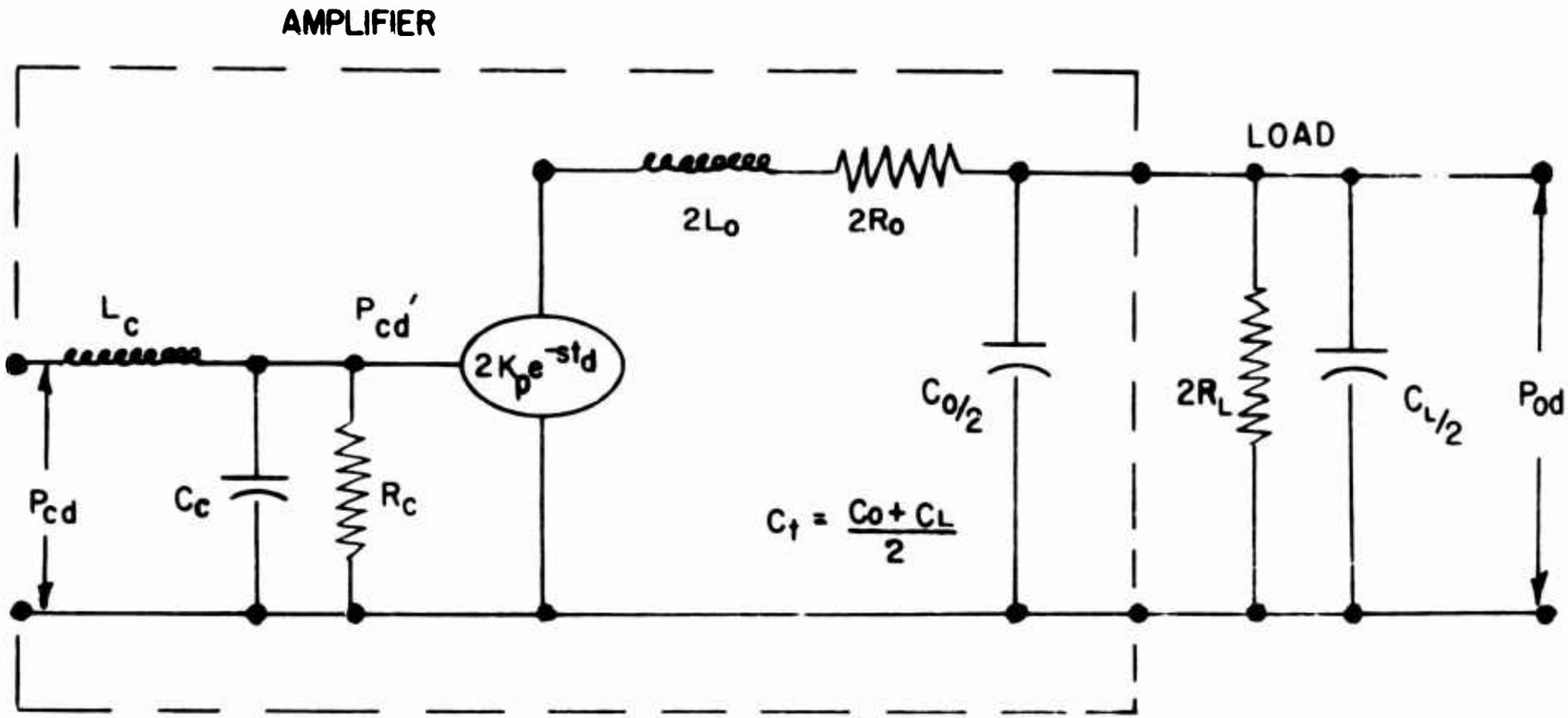

$$\frac{P_{od}}{P_{cd}} = \frac{2K_p R_L}{R_o + R_L} \cdot \frac{e^{-std}}{\left(1 + S\frac{L_c}{R_c} + S^2 L_c C_c\right)\left[1 + S\left(\frac{C_t 2R_o R_L}{R_o + R_L} + \frac{L_o}{R_o + R_L}\right) + S^2 \frac{2C_t L_o R_L}{R_o + R_L}\right]}$$

FIGURE 10 - EQUIVALENT CIRCUIT FOR VENTED JET INTERACTION AMPLIFIER.

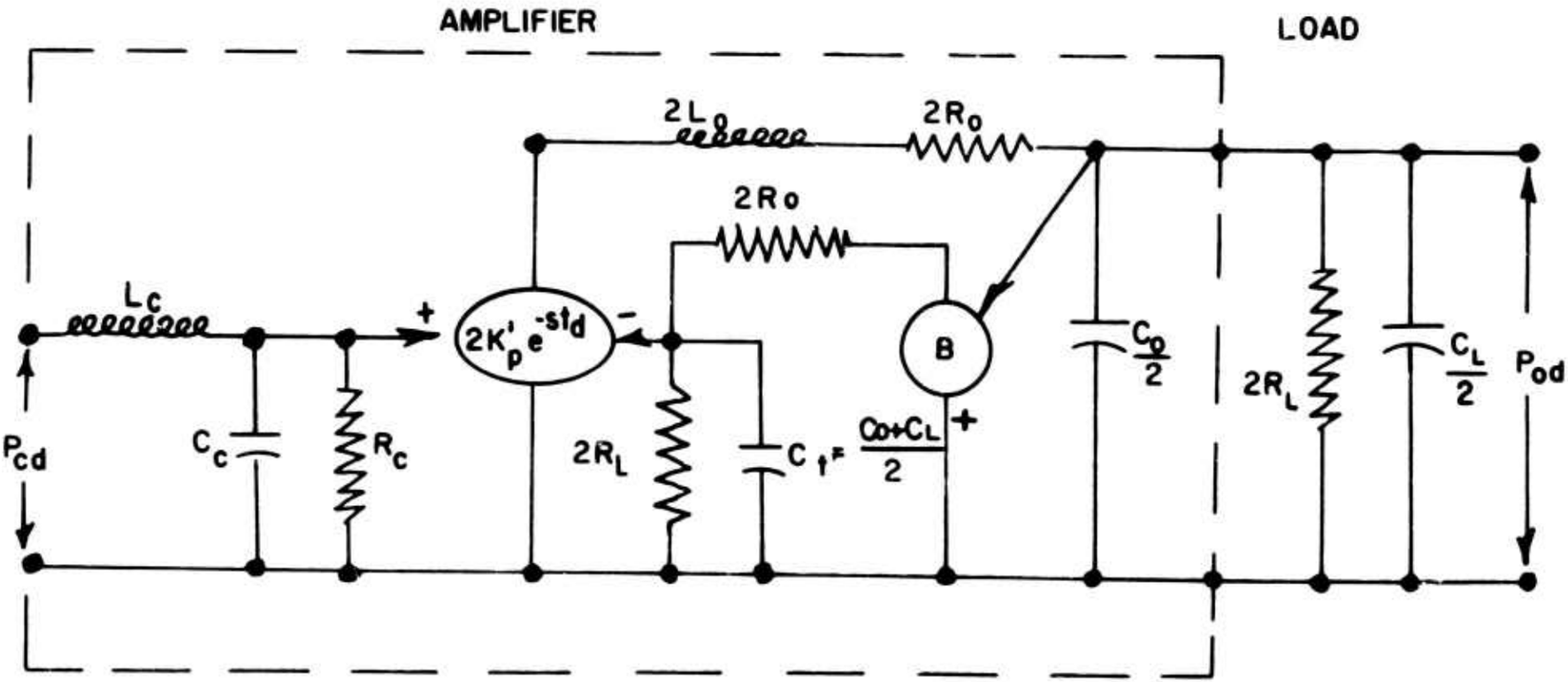

$$\frac{P_{od}}{P_{cd}} \approx \frac{2K_pR_L}{R_o+R_L} \frac{\left(1+SC_f\frac{2R_oR_L}{R_o+R_L}\right)e^{-std}}{\left(1+S\frac{L_c}{R_c}+S^2L_cR_c\right)\left[1+\frac{S\,4C_fR_oR_L}{(1+2K_pB)(R_o+R_L)}+\frac{S^2\,4C_f^2R_o^2R_L^2}{(1+2K_pB)(R_o+R_L)^2}+\frac{S^3\,4L_oC_f^2R_L^2R_o}{(1+2K_pB)(R_o+R_L)^2}\right]}$$

WHERE $K_p = K_p'/(1+2K_p'B)$ THAT IS, THE ACTUAL MEASURED AMPLIFICATION FACTOR

FIGURE 11 - EQUIVALENT CIRCUIT FOR CLOSED JET INTERACTION AMPLIFIER

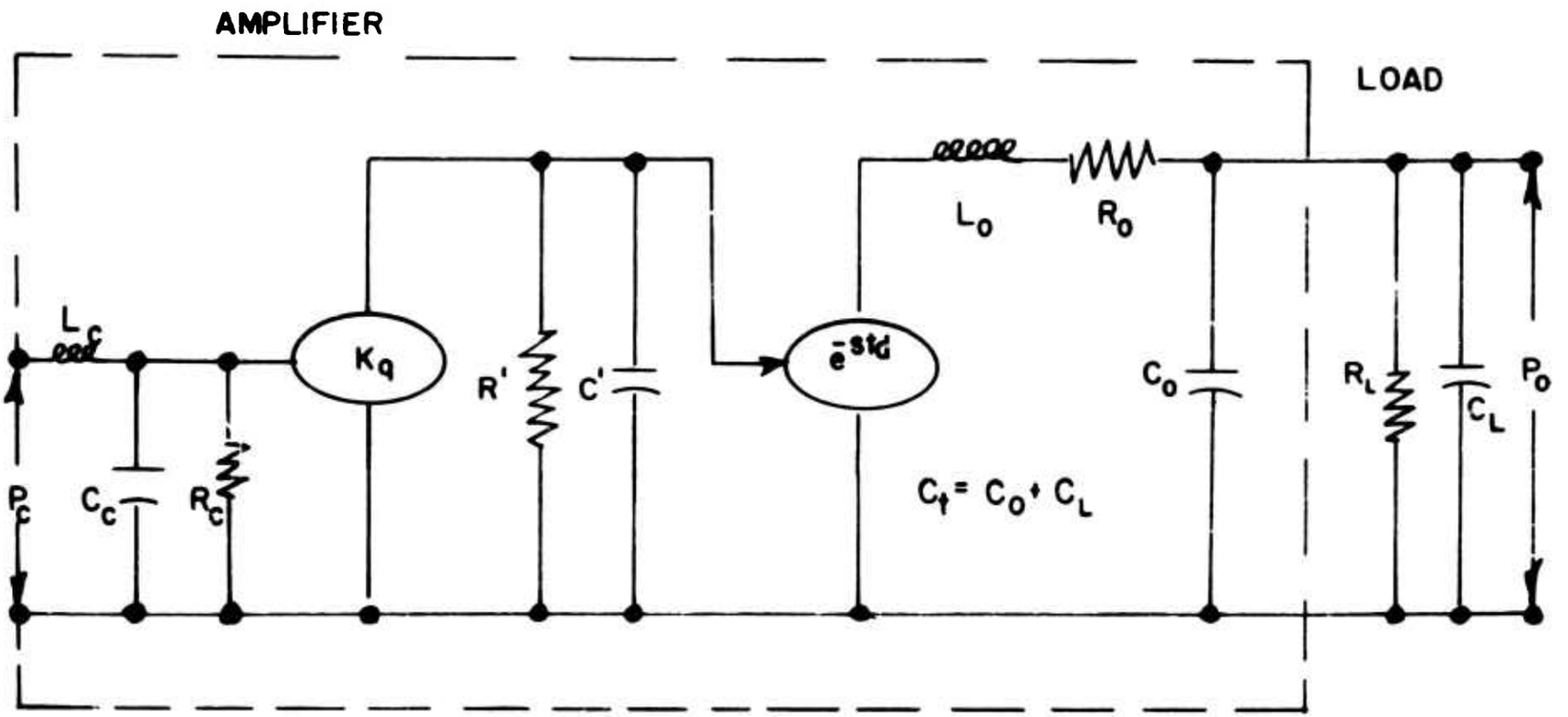

$$\frac{P_o}{P_c} = \frac{K_q R' R_L}{R_c(R_o+R_L)} \frac{e^{-st_d}}{\left(1+S\frac{L_c}{R_c}+S^2L_cC_c\right)\left(1+SC'R'\right)\left[1+S\left(\frac{C_tR_oR_L+L_o}{R_o+R_L}\right)+S^2\frac{L_oC_tR_L}{R_o+R_L}\right]}$$

FIGURE 12- EQUIVALENT CIRCUIT FOR VENTED ELBOW AMPLIFIER

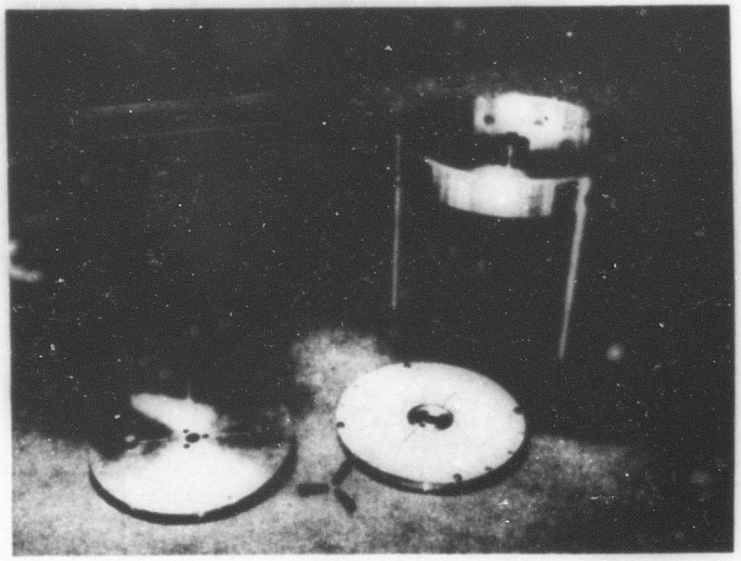

a.) PNEUMATIC FUNCTION GENERATOR AND ACCESSORIES.

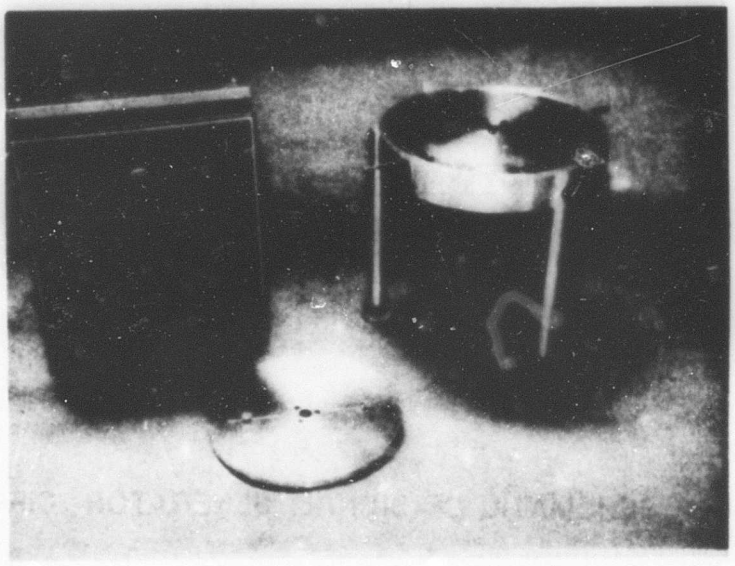

b.) PNEUMATIC FUNCTION GENERATOR WITH FREQUENCY DISC IN PLACE.

FIGURE 13 - PHOTOS OF SINUSOIDAL SIGNAL GENERATOR.

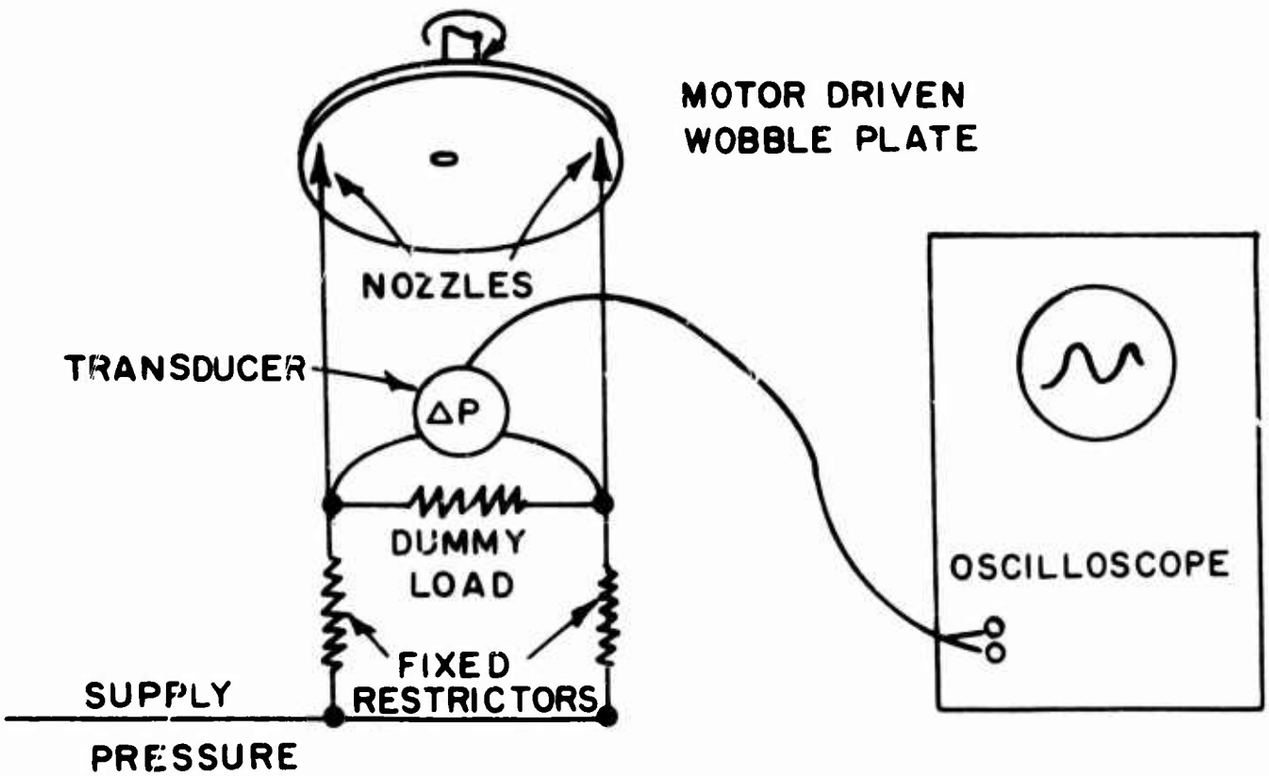

FIGURE 14 - SCHEMATIC OF SIGNAL GENERATOR CIRCUIT.

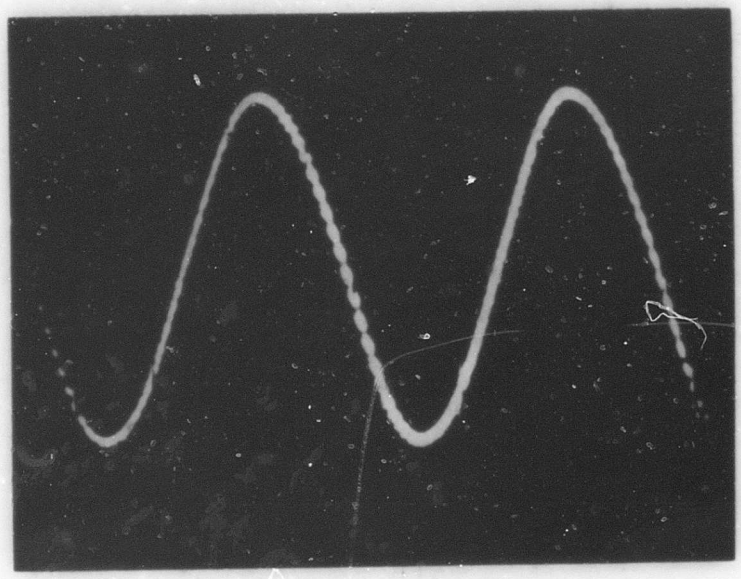

a.) 1-1/4 CYCLES PER SECOND

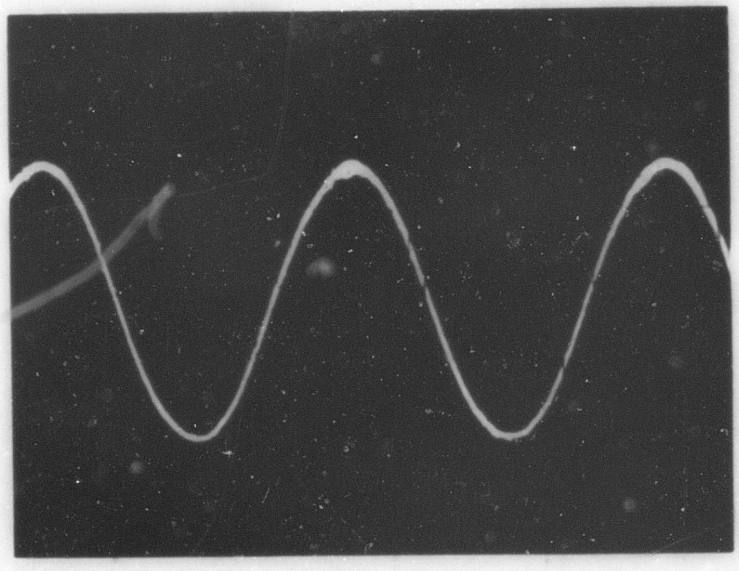

b.) 320 CYCLES PER SECOND

FIGURE 15 - TYPICAL SIGNALS GENERATED BY SINUSOIDAL SIGNAL GENERATOR.

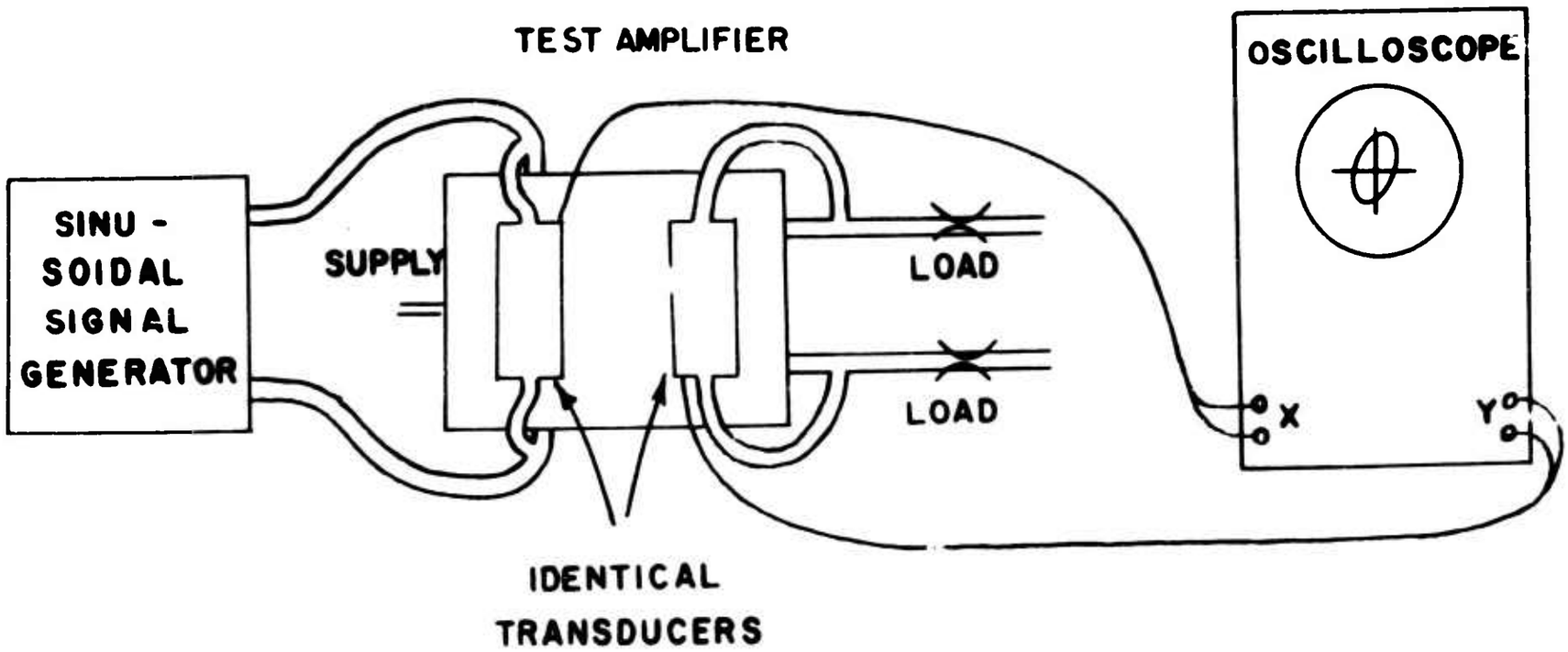

FIGURE 16 - TEST CIRCUIT FOR VENTED JET INTERACTION AMPLIFIER.

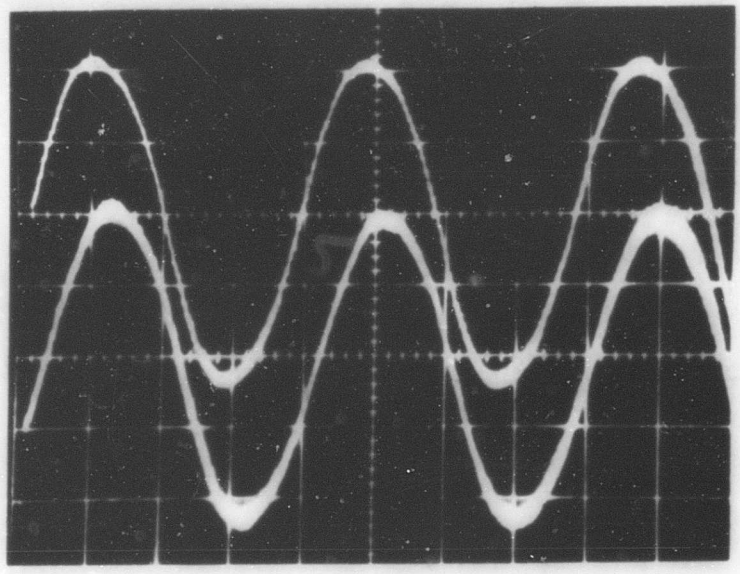

a.) INPUT SIGNAL (TOP TRACE) AND OUTPUT SIGNAL AT 50 CPS.

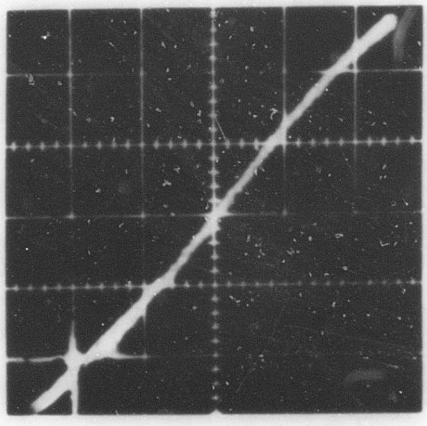

b.) INPUT VERSUS OUTPUT AT 5 CPS.

c.) INPUT VERSUS OUTPUT AT 50 CPS (SHOWING PHASE LAG).

FIGURE 17 - TYPICAL DATA RECORDED FROM FREQUENCY RESPONSE TESTS.

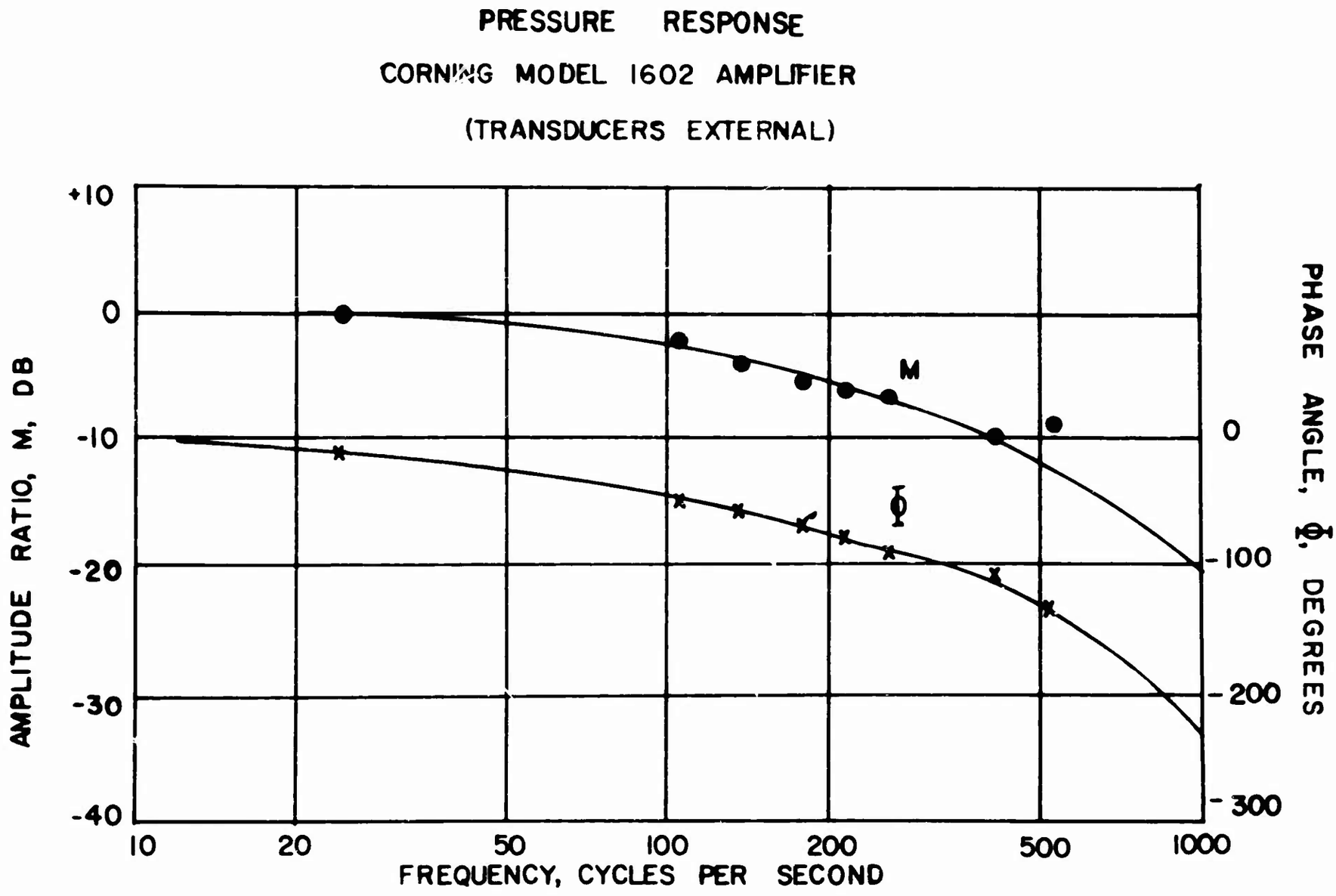

FIGURE 18- EXPERIMENTAL FREQUENCY RESPONSE OF VENTED JET INTERACTION AMPLIFIER.

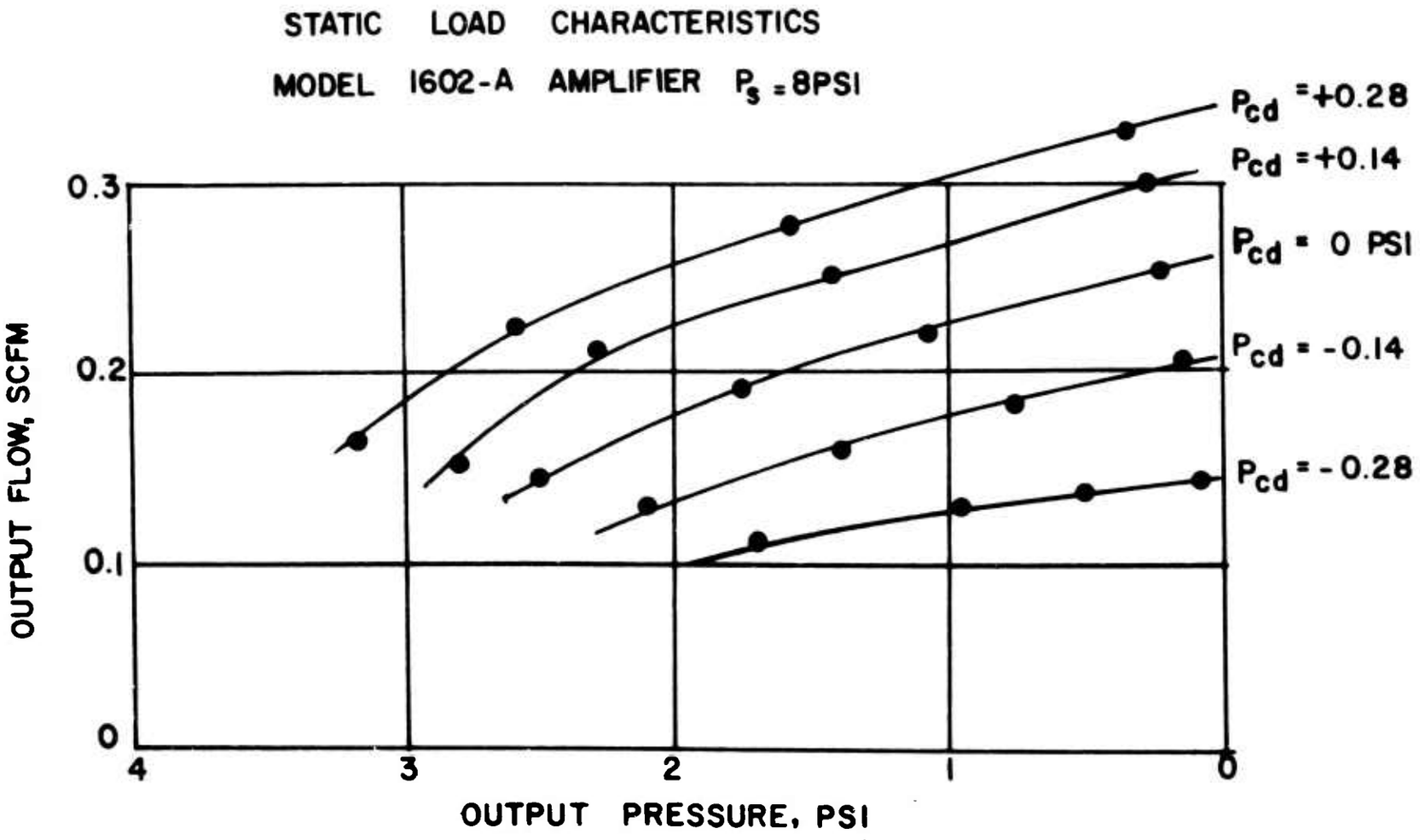

FIGURE 19 - OUTPUT CHARACTERISTICS OF VENTED JET INTERACTION AMPLIFIER.

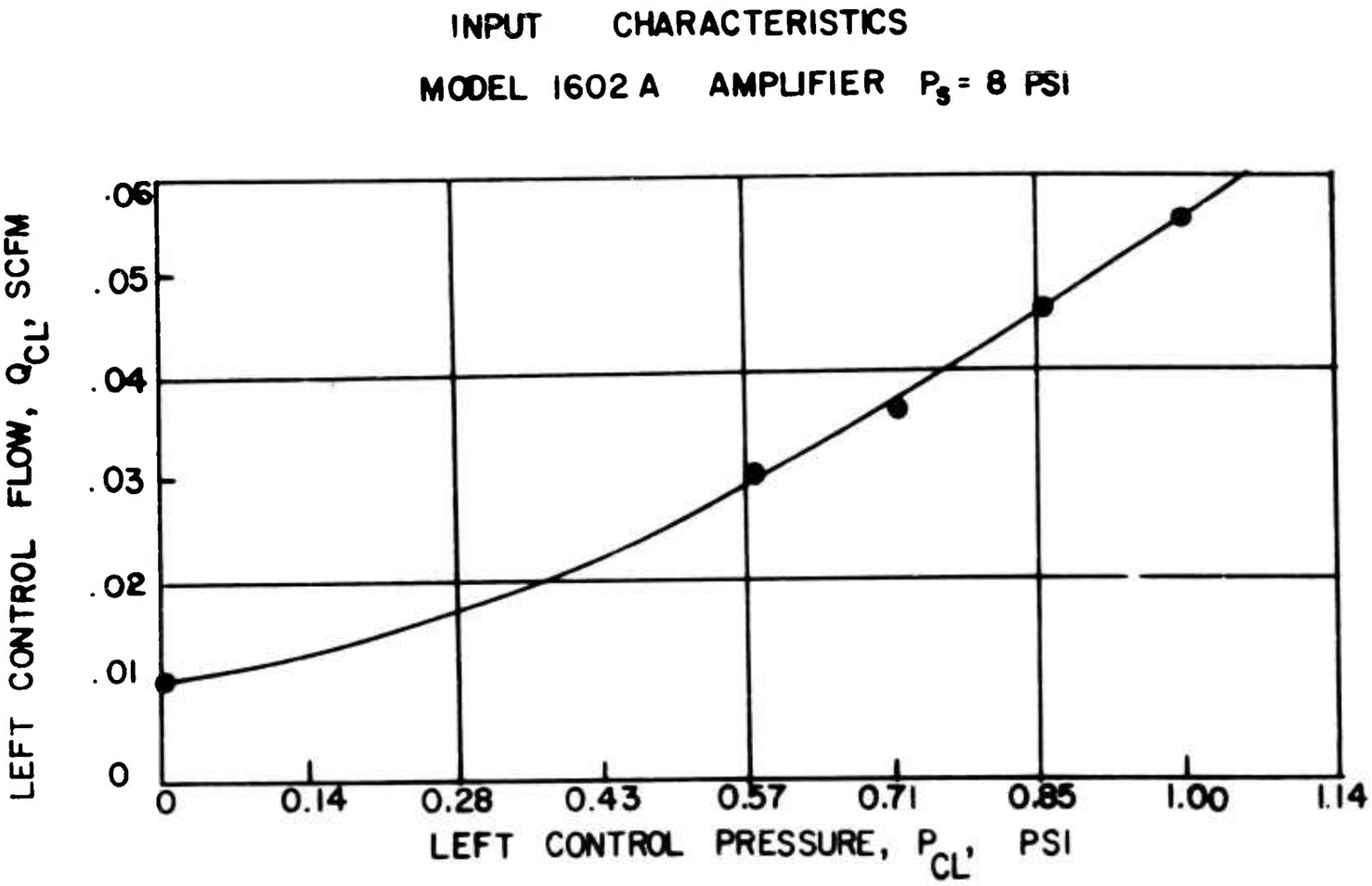

FIGURE 20 - INPUT CHARACTERISTICS OF VENTED JET INTERACTION AMPLIFIER.

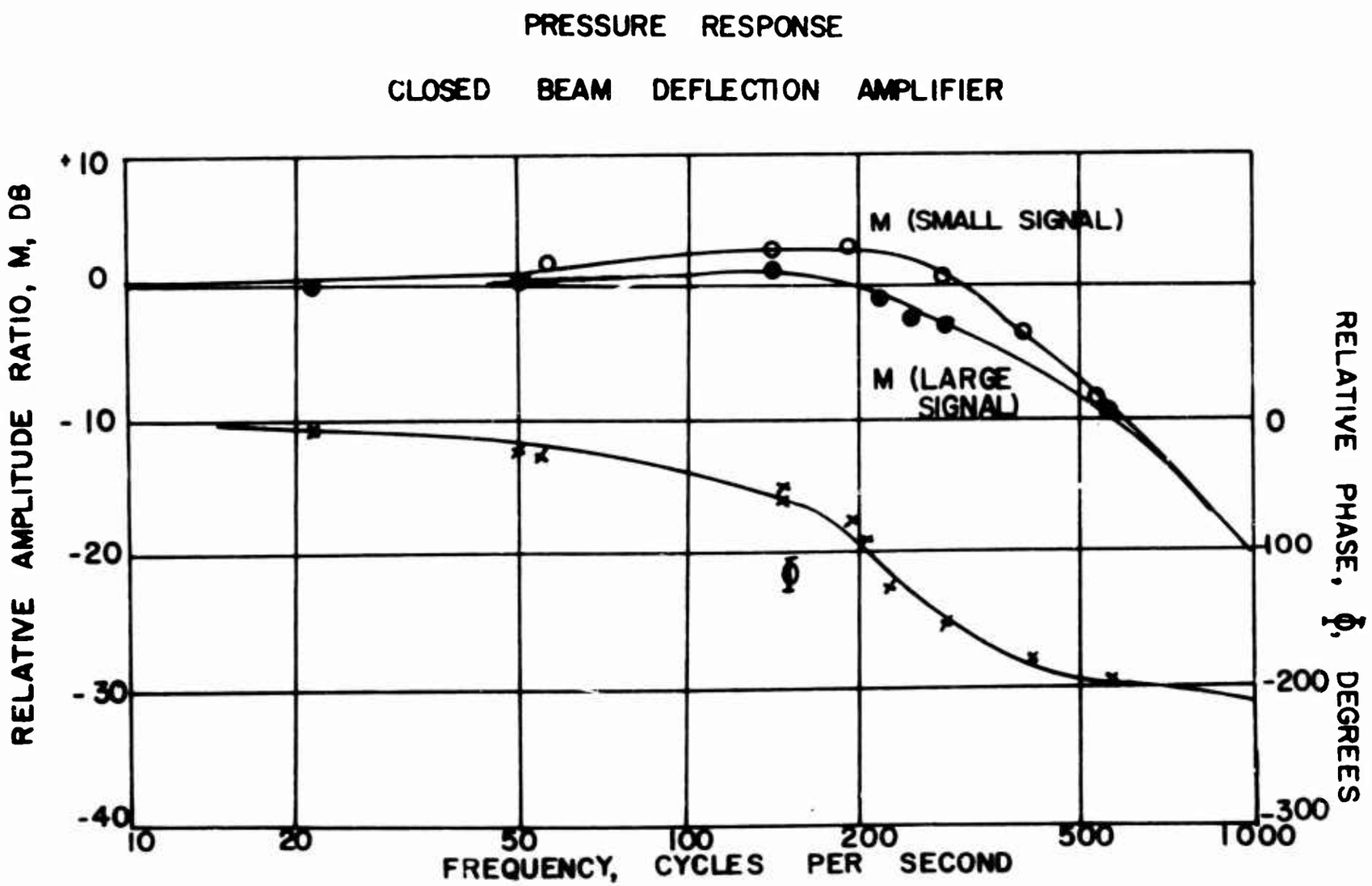

FIGURE 21 - EXPERIMENTAL FREQUENCY RESPONSE OF CLOSED JET INTERACTION AMPLIFIER.

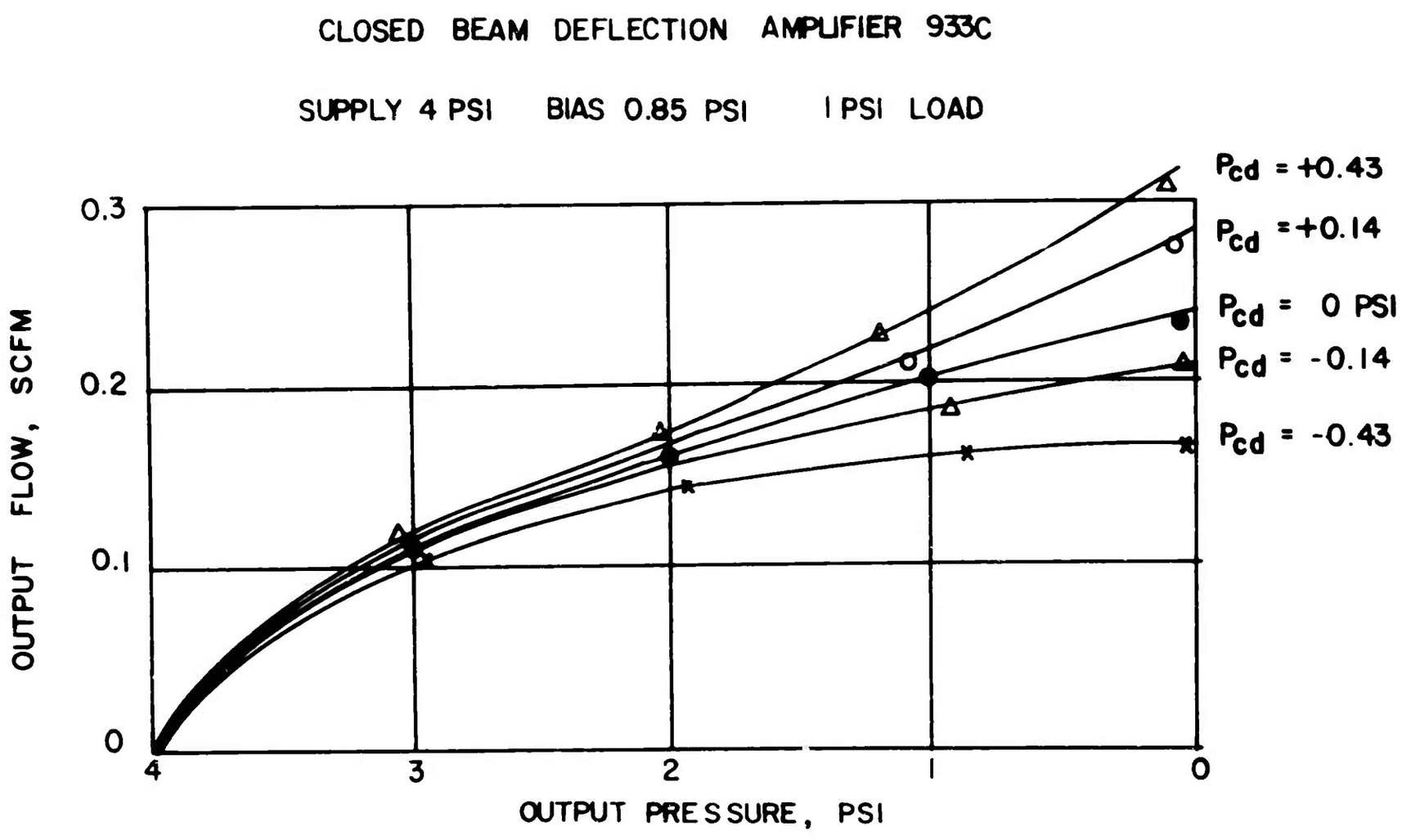

FIGURE 22 - OUTPUT CHARACTERISTICS OF CLOSED JET INTERACTION AMPLIFIER.

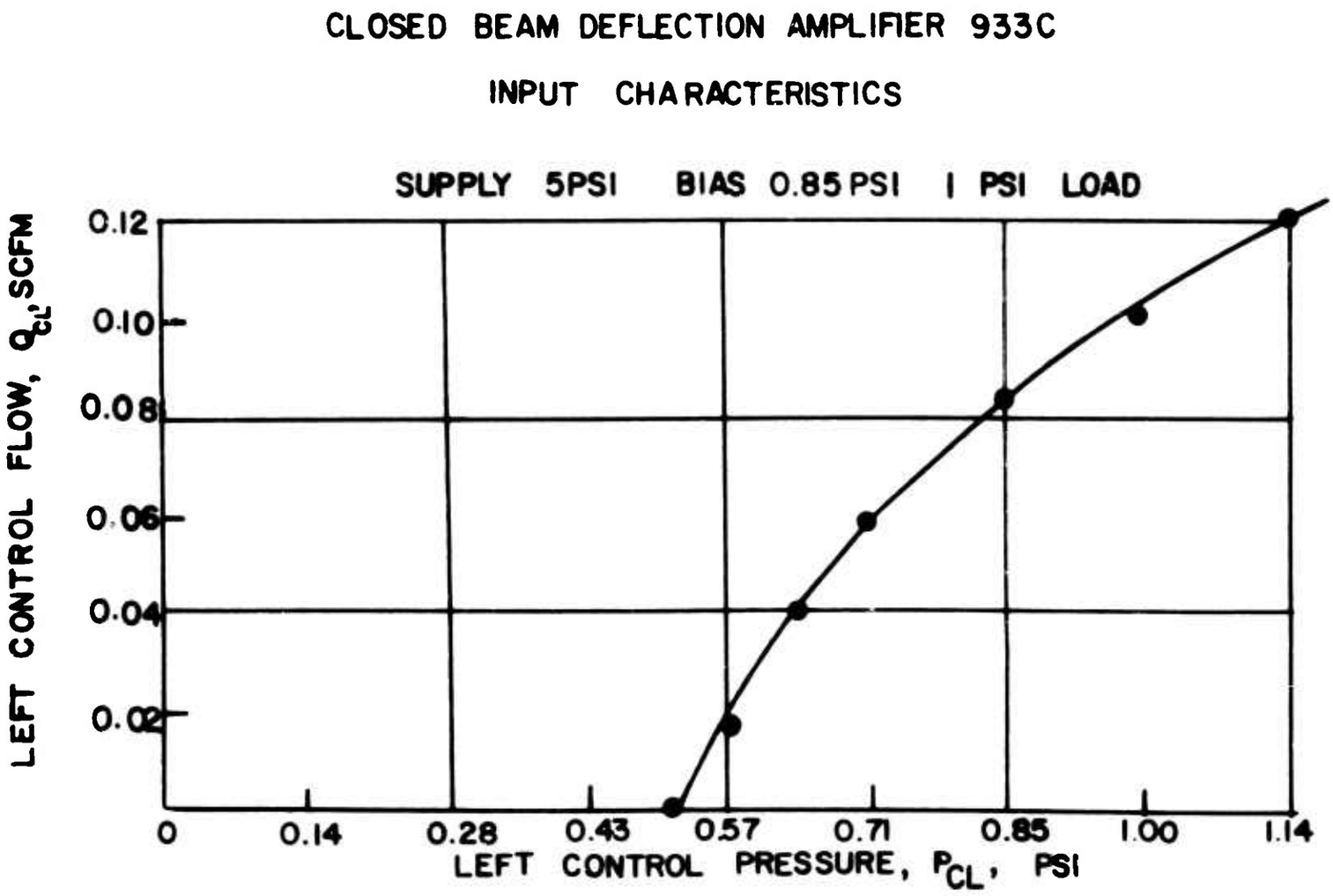

FIGURE 23 - INPUT CHARACTERISTICS OF CLOSED JET INTERACTION AMPLIFIER.

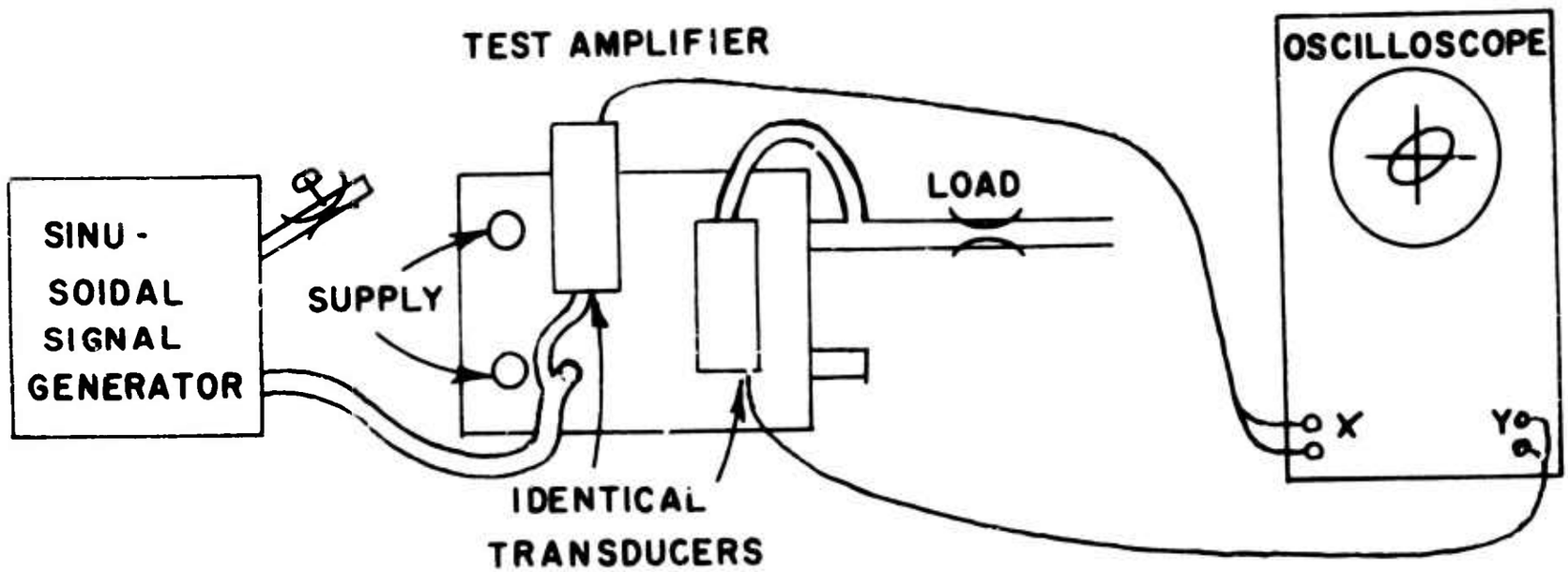

FIGURE 24 - TEST CIRCUIT FOR VENTED ELBOW AMPLIFIER.

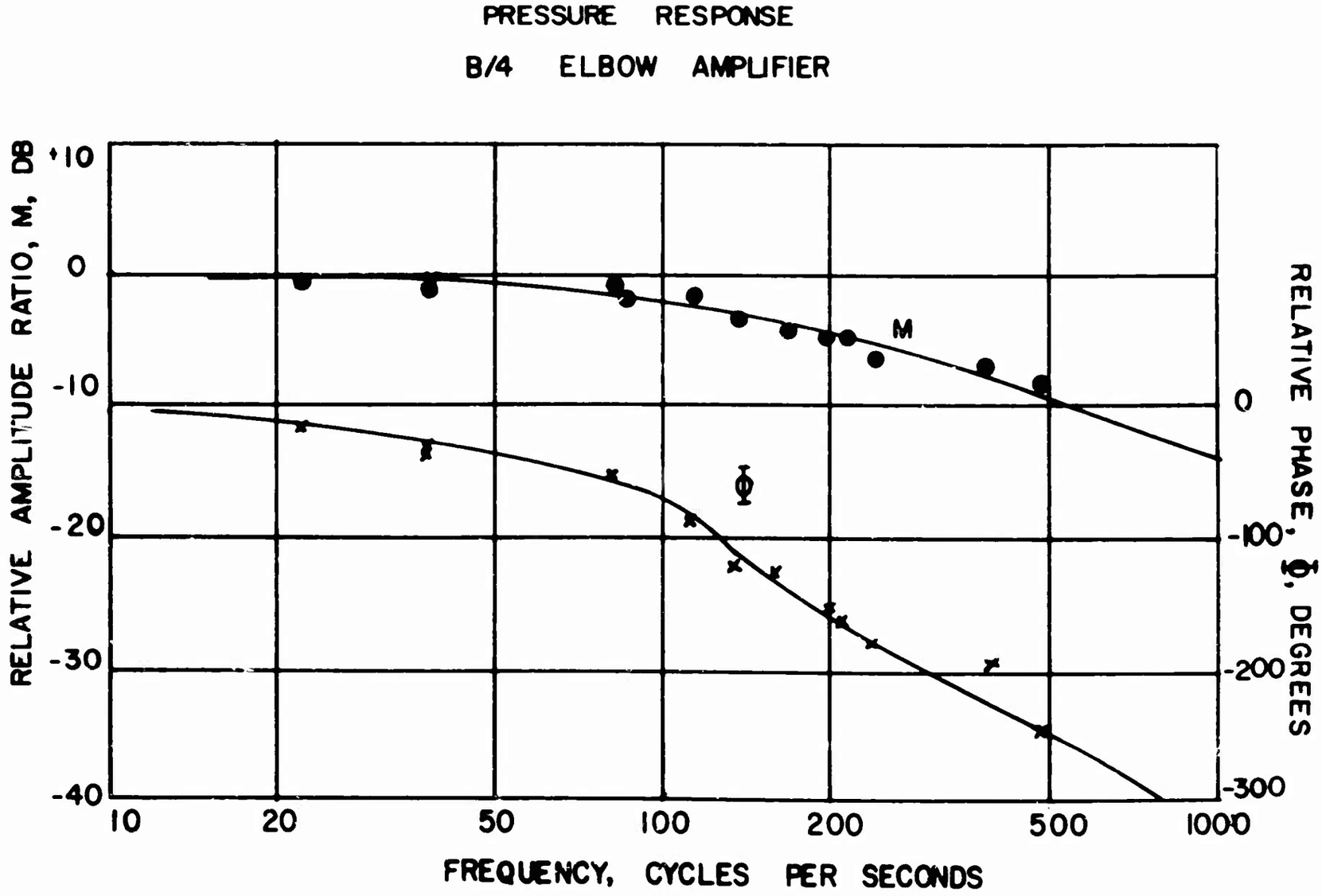

FIGURE 25 - EXPERIMENTAL FREQUENCY RESPONSE OF VENTED ELBOW AMPLIFIER.

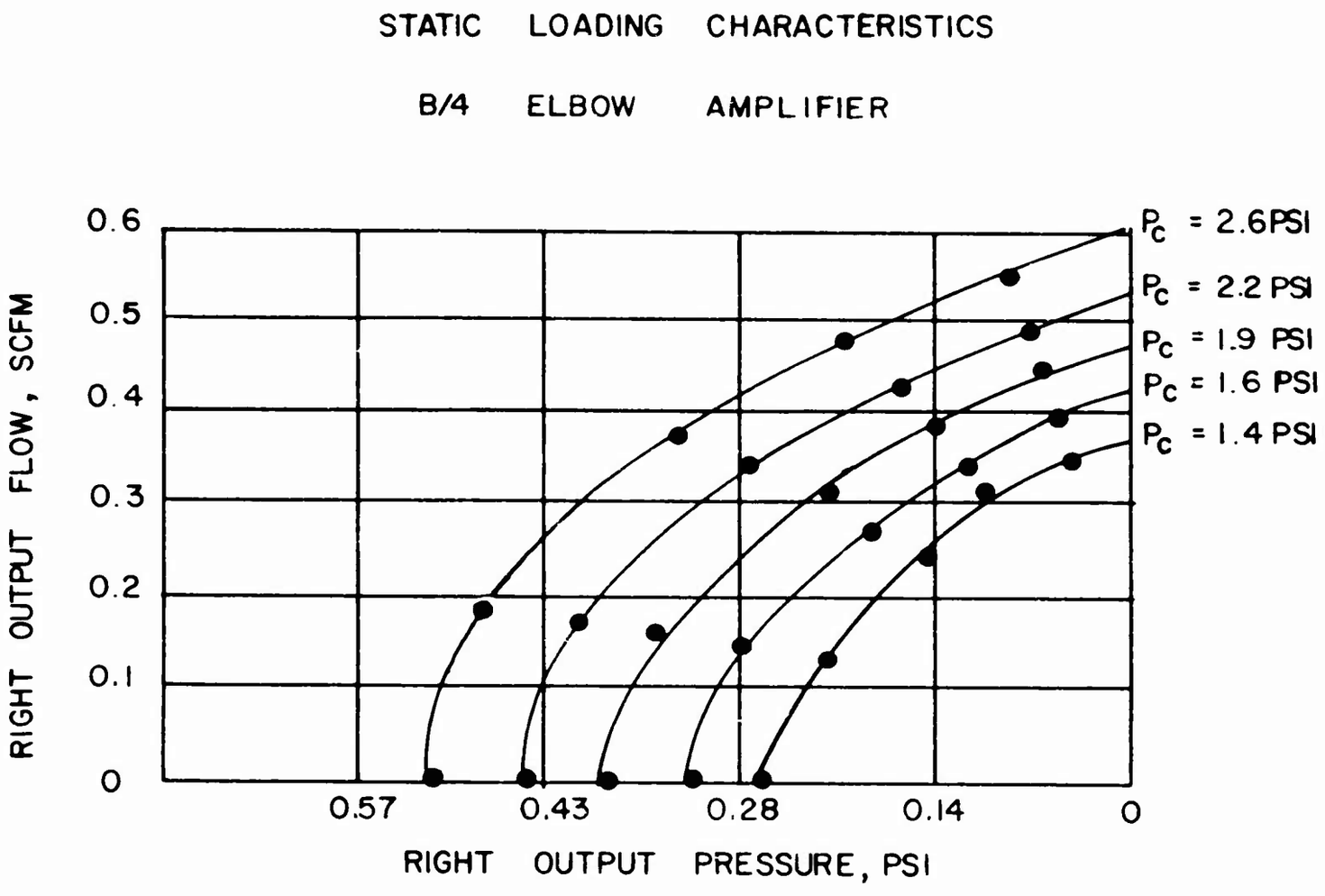

FIGURE 26 - OUTPUT CHARACTERISTICS OF VENTED ELBOW AMPLIFIER.

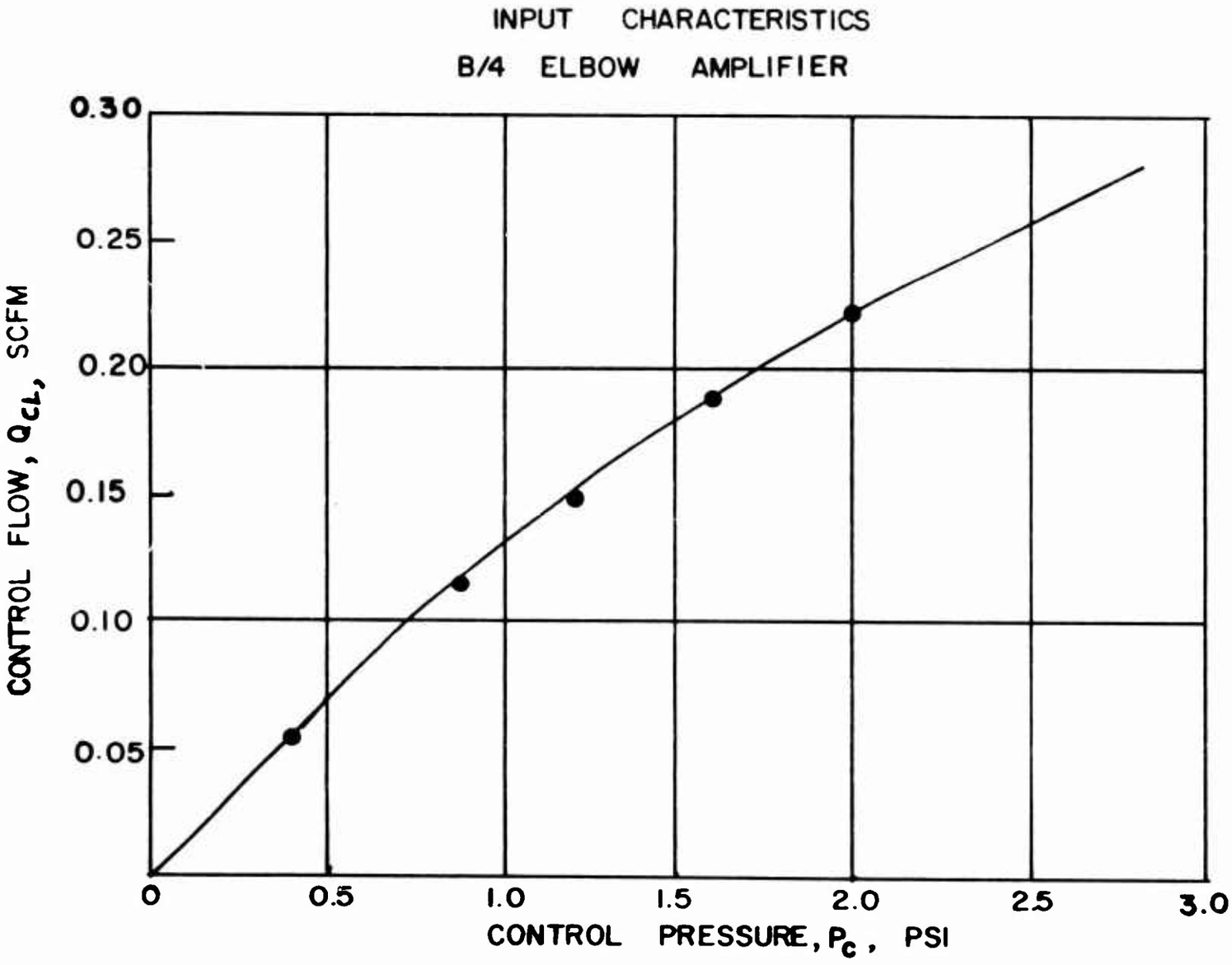

FIGURE 27- INPUT CHARACTERISTICS OF VENTED ELBOW AMPLIFIER.

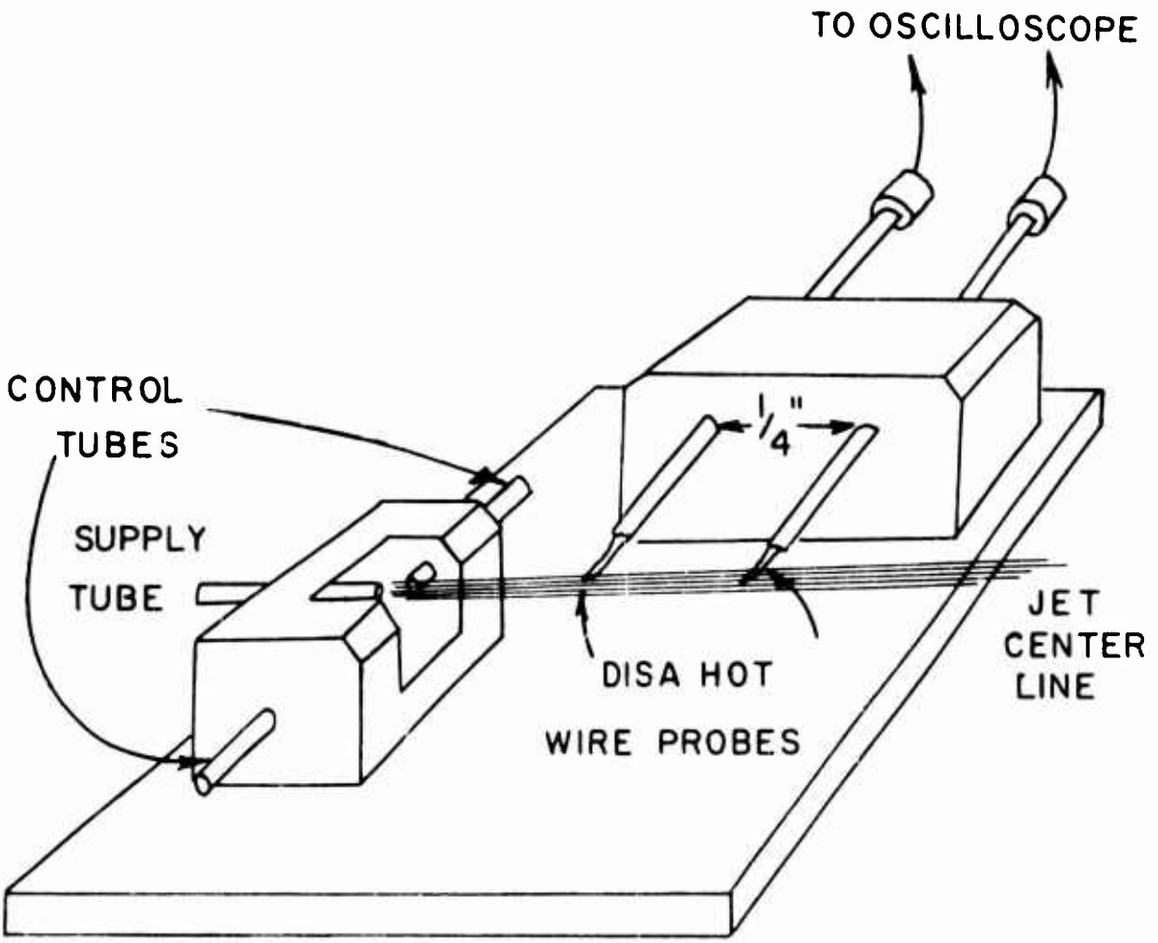

FIGURE 28 - EXPERIMENTAL APPARATUS FOR TESTING BEAM DYNAMICS

TWO - DIMENSIONAL BEAM DEFLECTION TEST

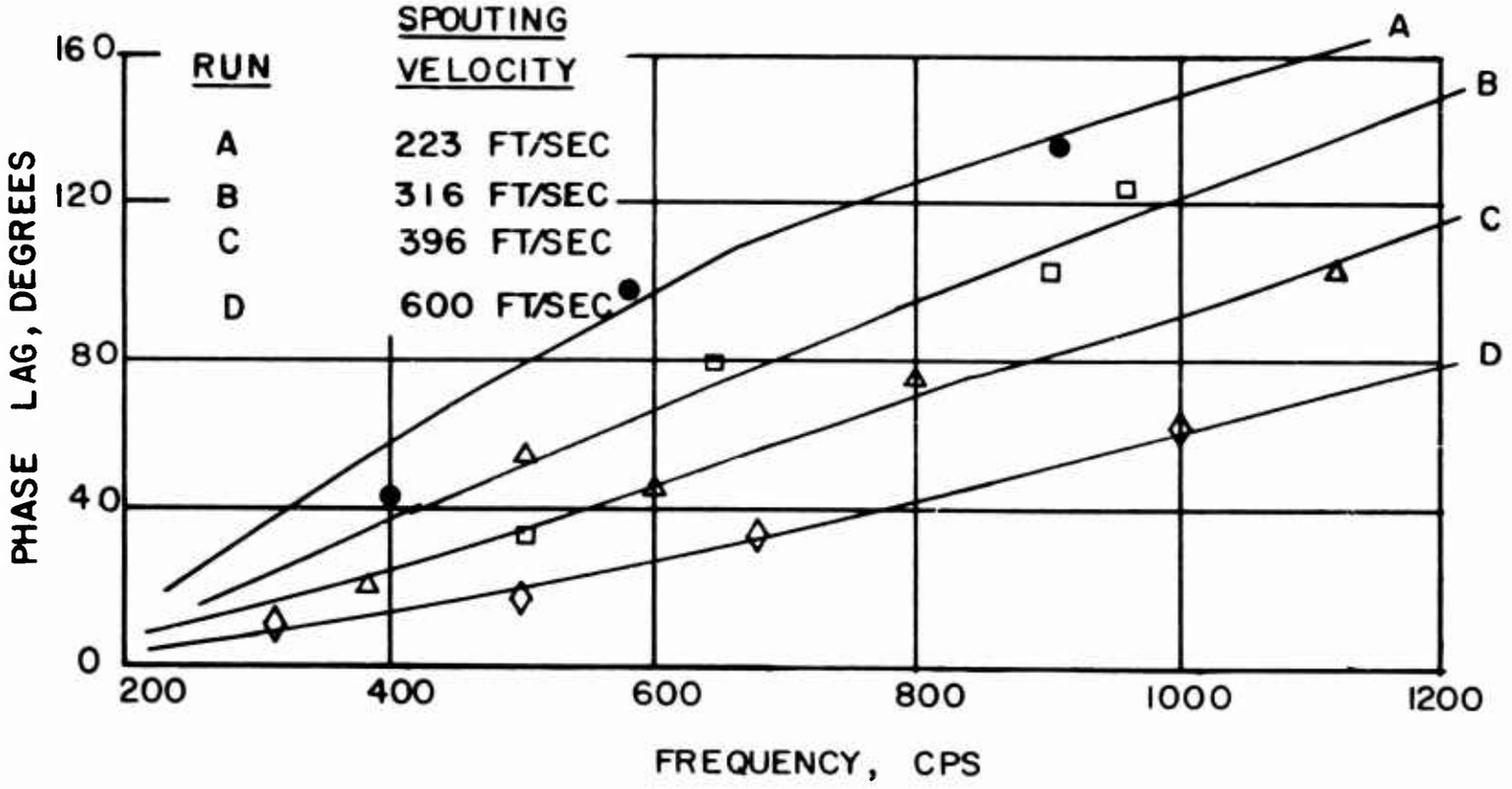

FIGURE 29 - RESULTS OF BEAM DYNAMICS TESTS.

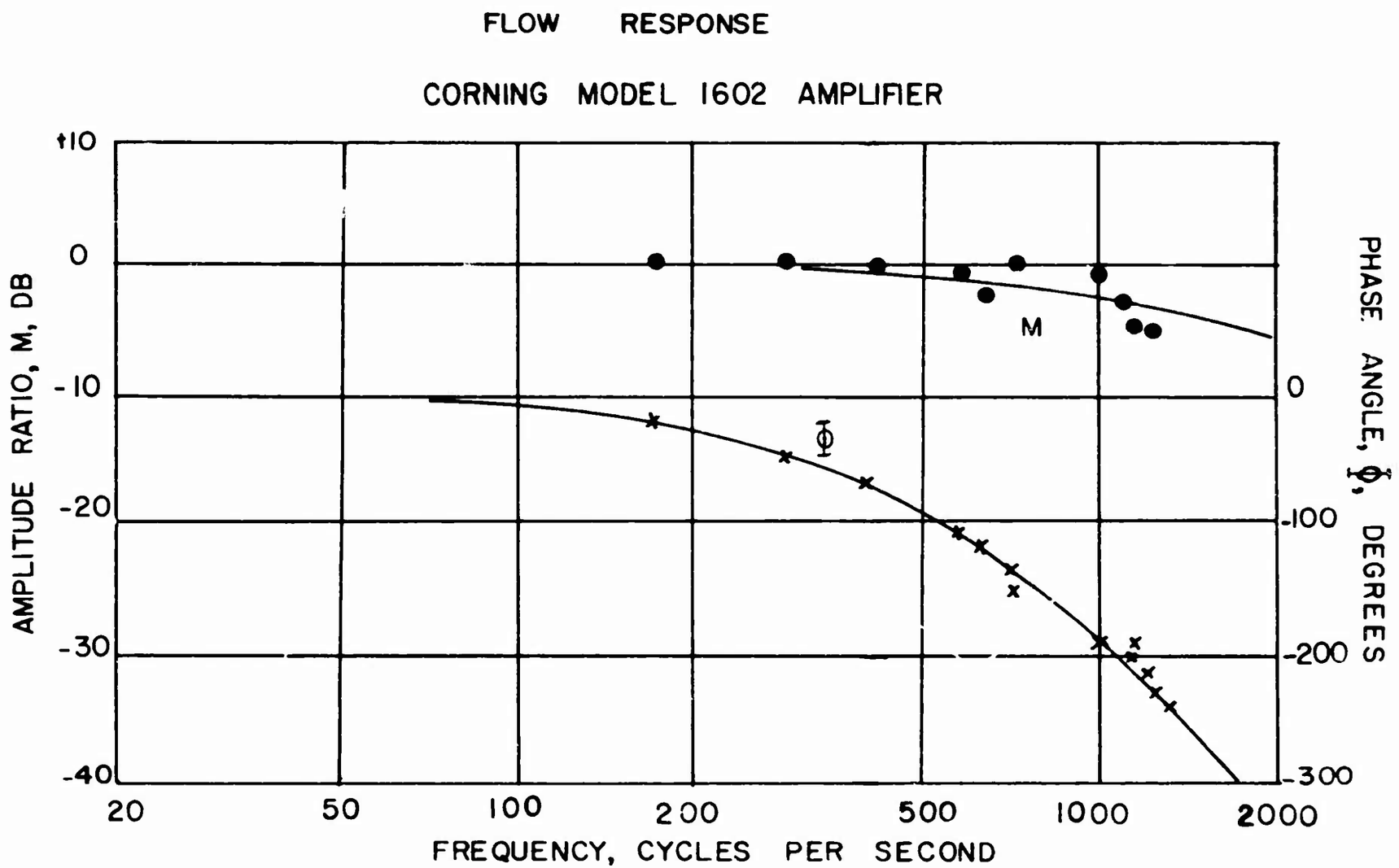

FIGURE 30 - FLOW RESPONSE OF JET INTERACTION AMPLIFIER USING HOT-WIRE SENSORS.

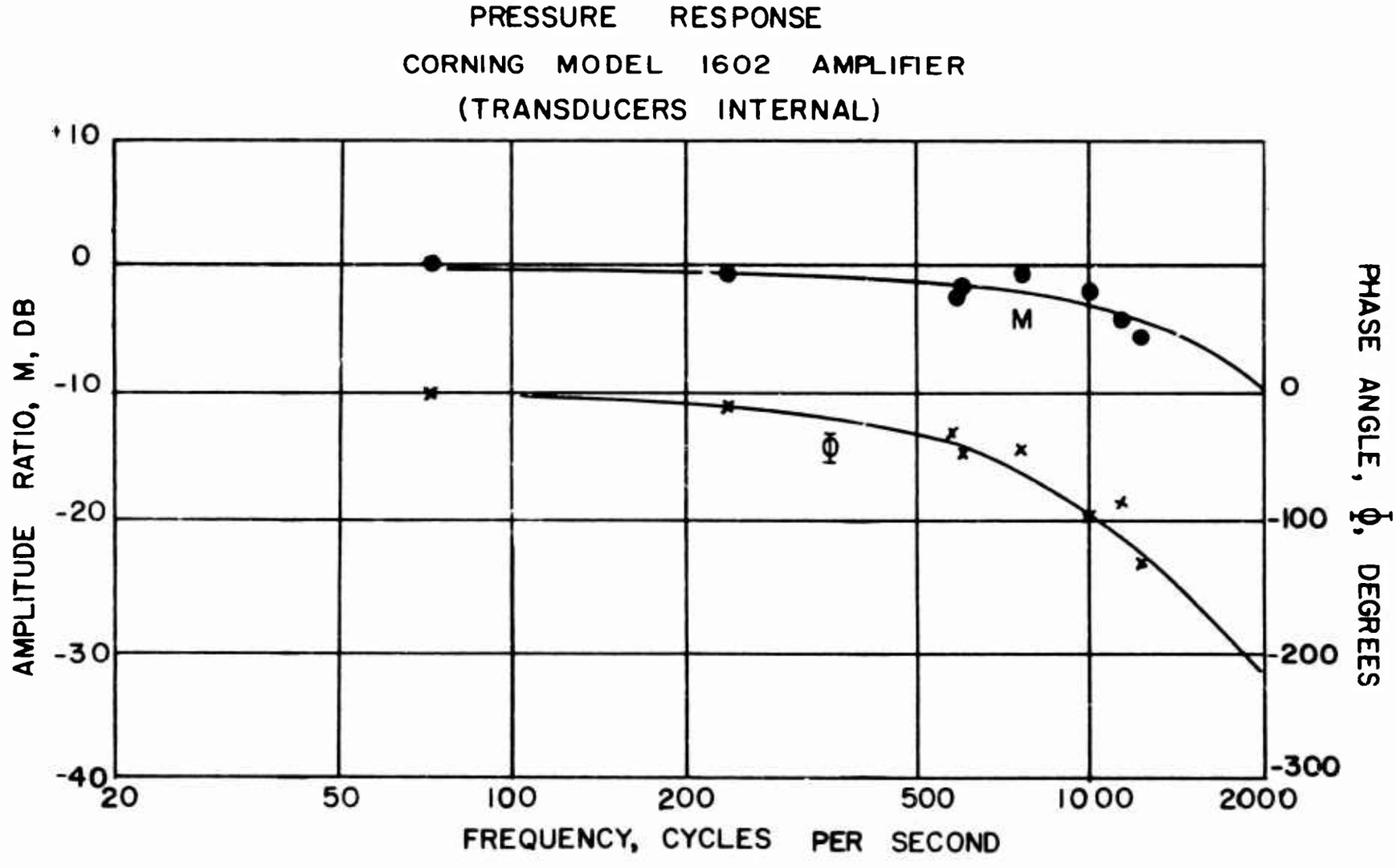

FIGURE 31 - PRESSURE RESPONSE OF JET INTERACTION AMPLIFIER USING INTERNAL PRESSURE SENSORS.

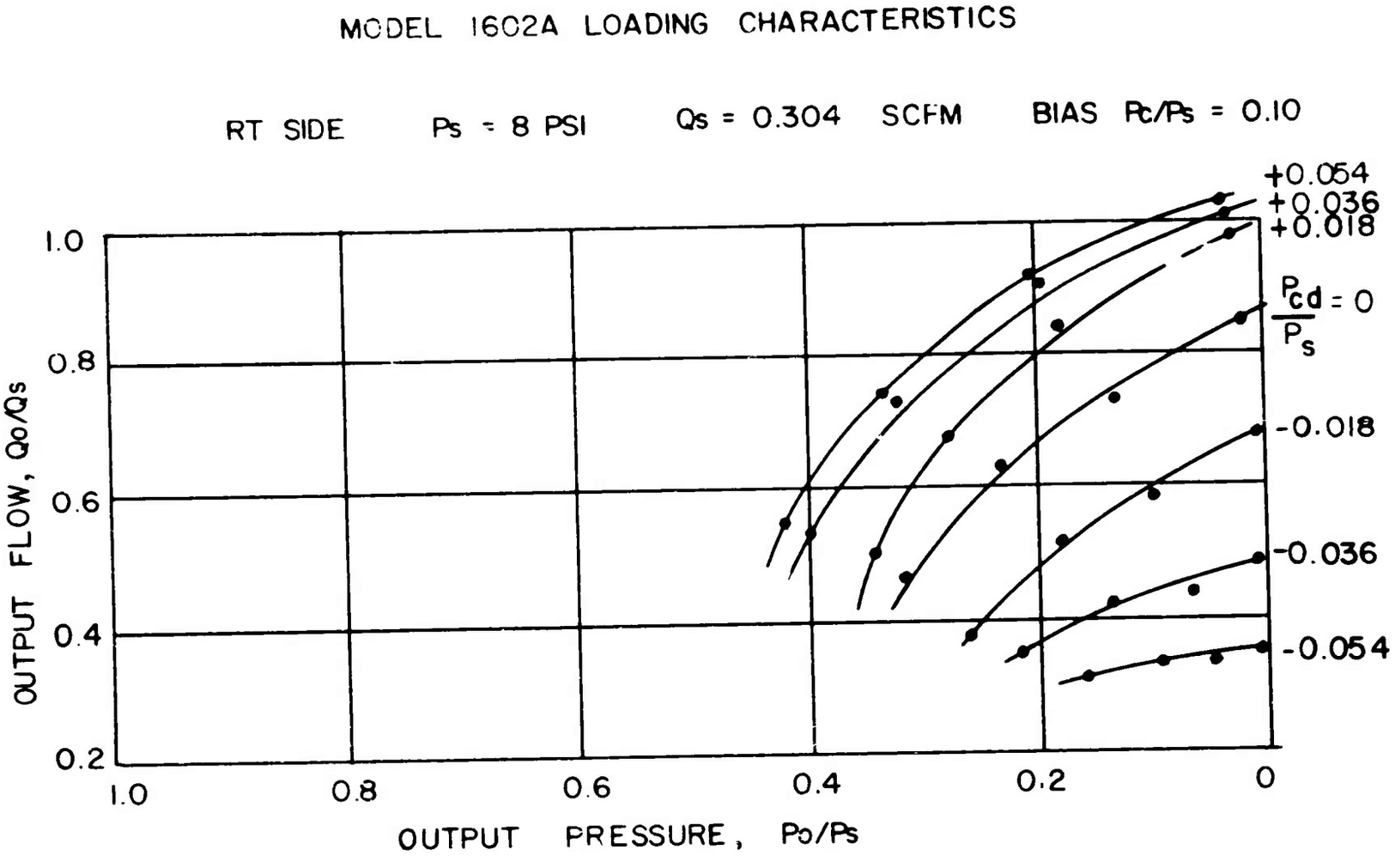

FIGURE 32 - NORMALIZED OUTPUT CHARACTERISTICS OF MODEL 1602A AT 8 PSI.

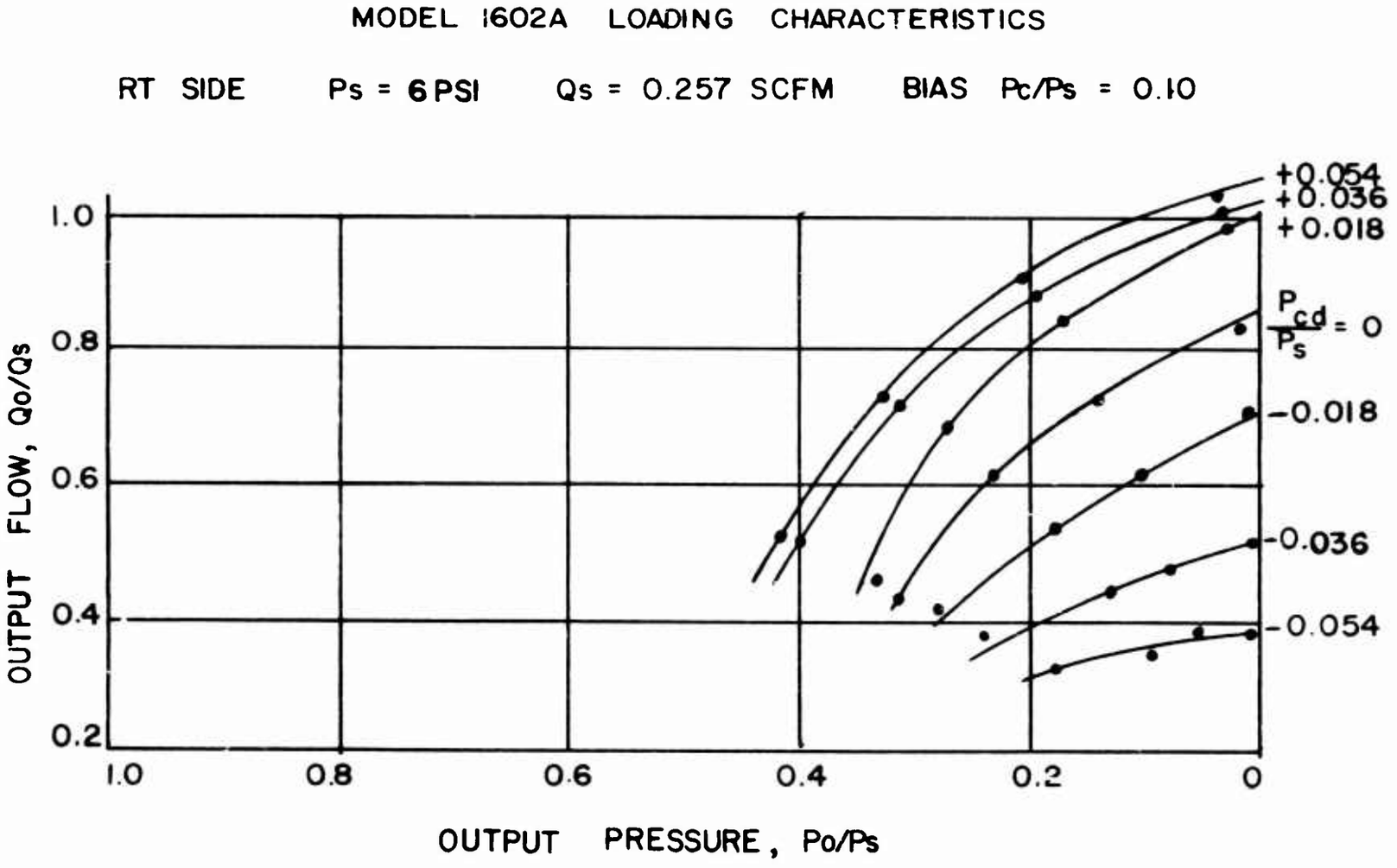

FIGURE 33 - NORMALIZED OUTPUT CHARACTERISTICS OF MODEL 1602A AT 6 PSI.

MODEL 1602A LOADING CHARACTERISTICS

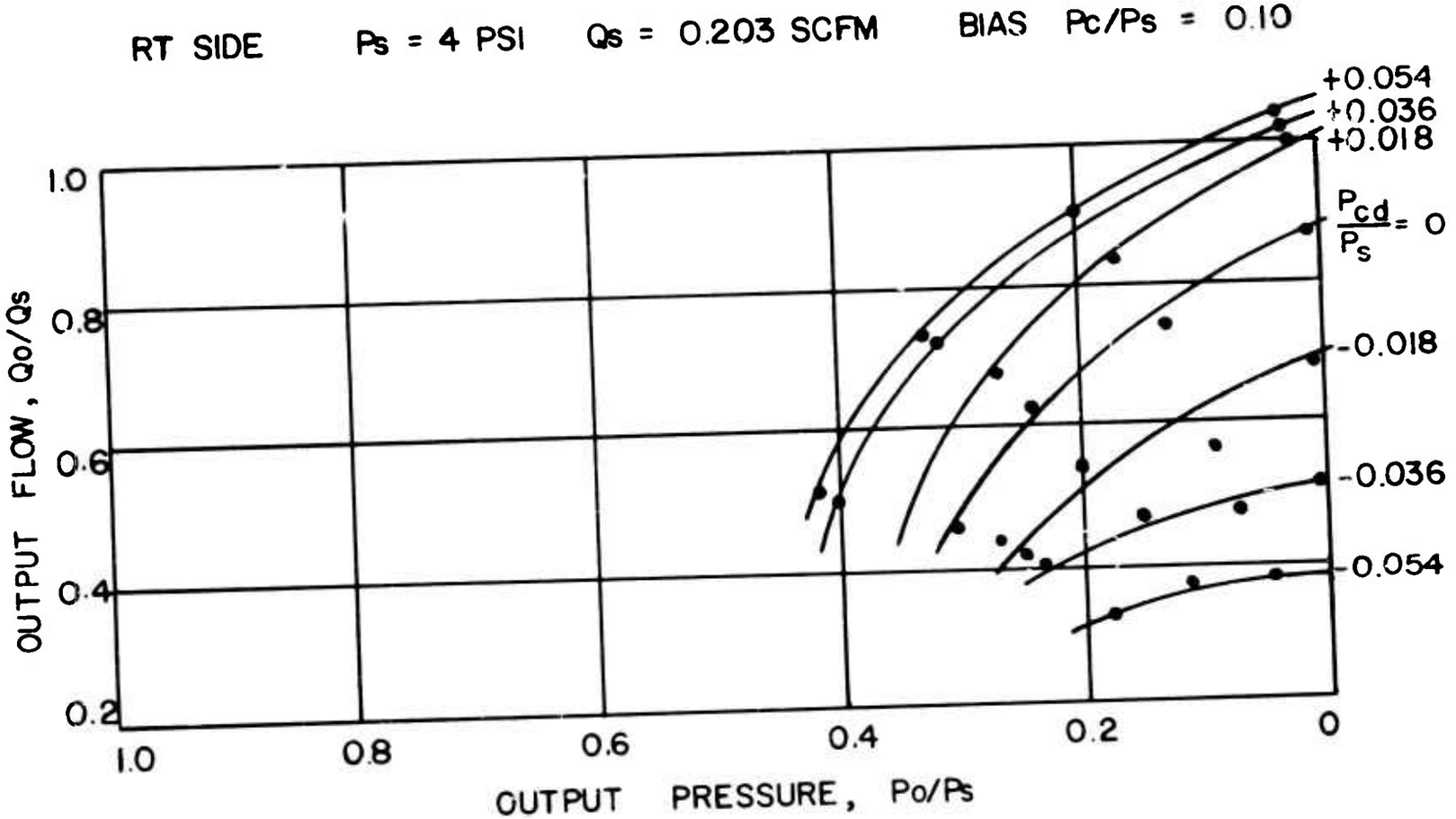

FIGURE 34 - NORMALIZED OUTPUT CHARACTERISTICS OF MODEL 1602A AT 4 PSI.

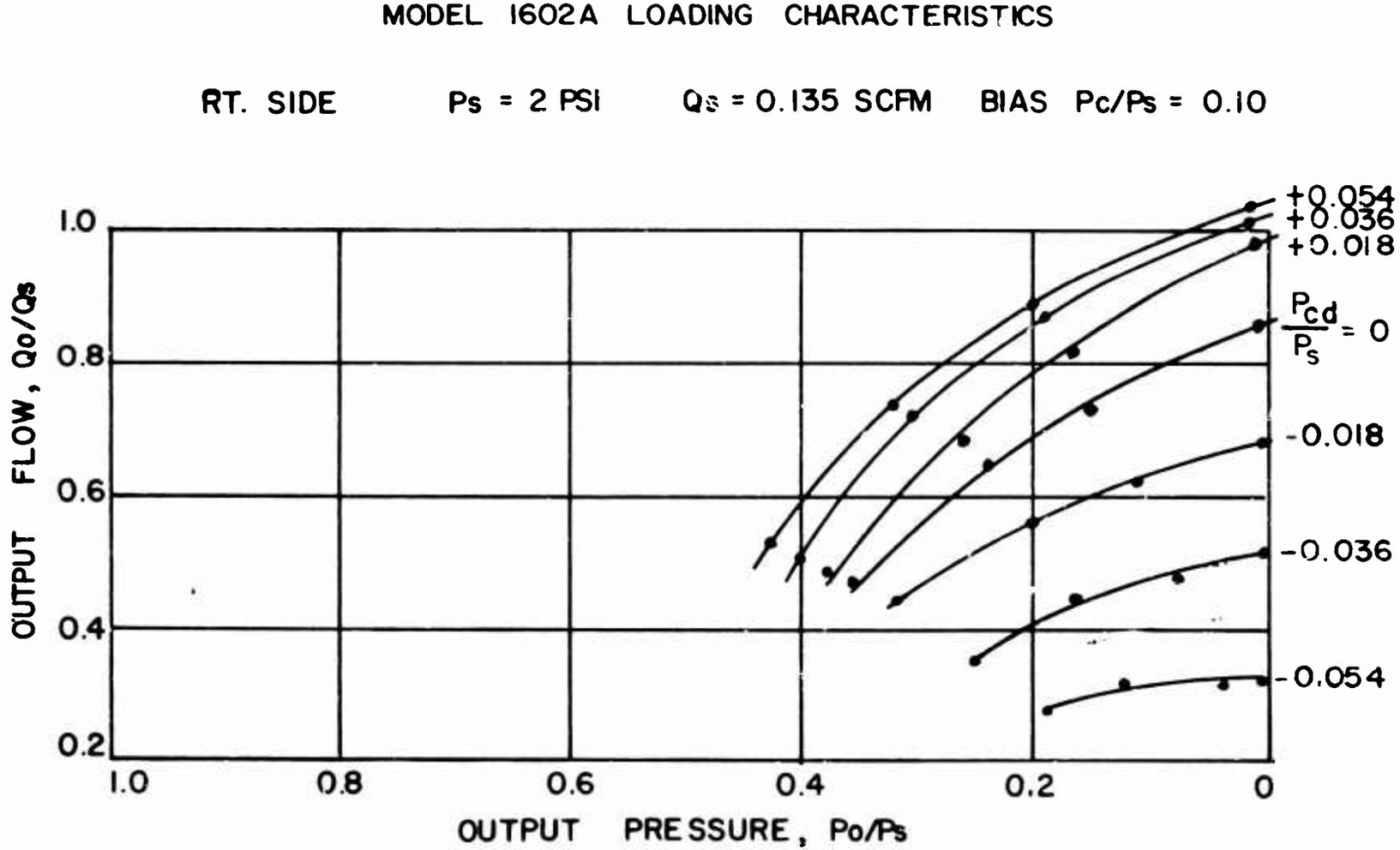

FIGURE 35 - NORMALIZED OUTPUT CHARACTERISTICS OF MODEL 1602A AT 2PSI.

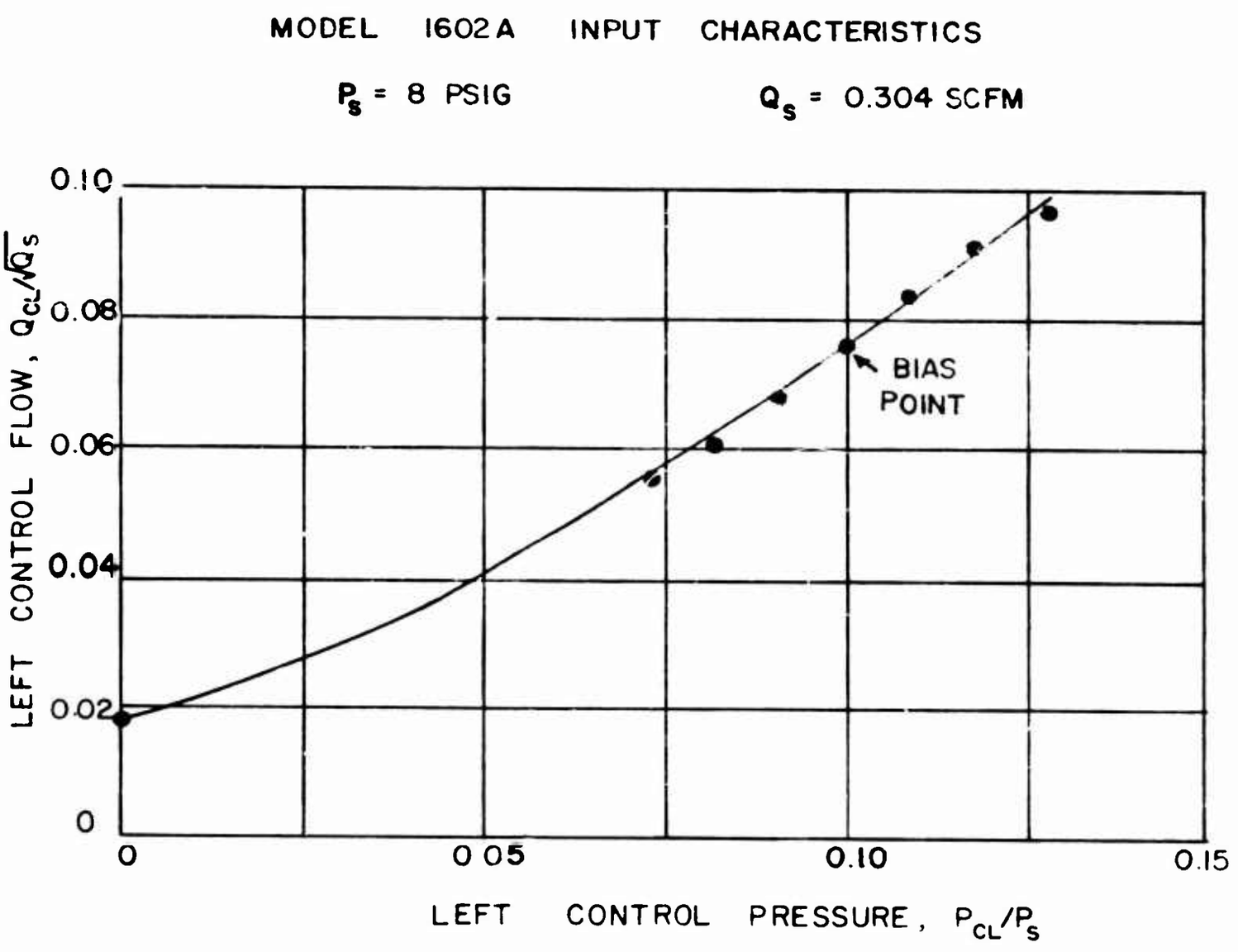

FIGURE 36 - NORMALIZED INPUT CHARACTERISTICS OF MODEL 1602A AT 8 PSI.

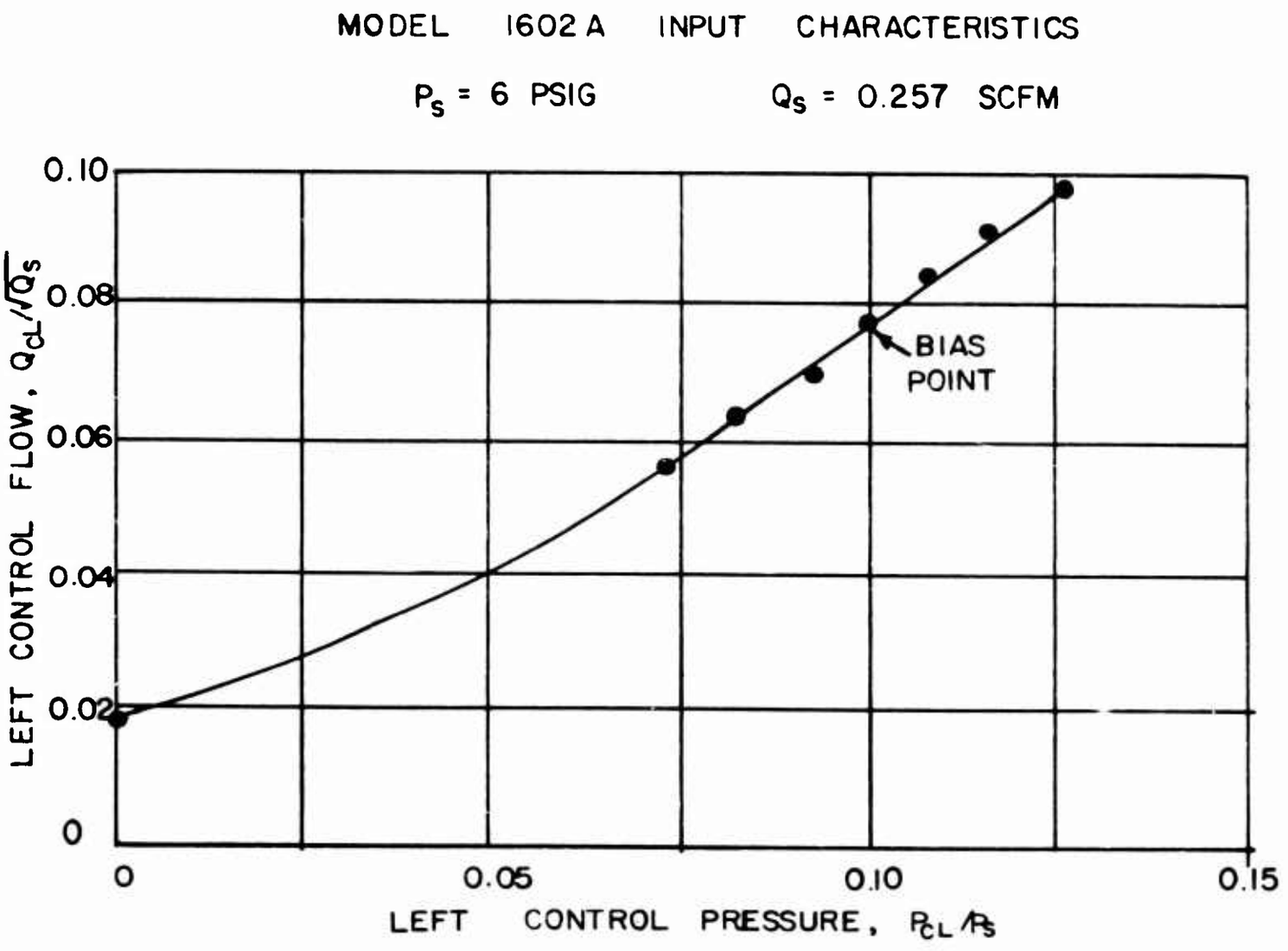

FIGURE 37 - NORMALIZED INPUT CHARACTERISTICS OF MODEL 1602A AT 6 PSI.

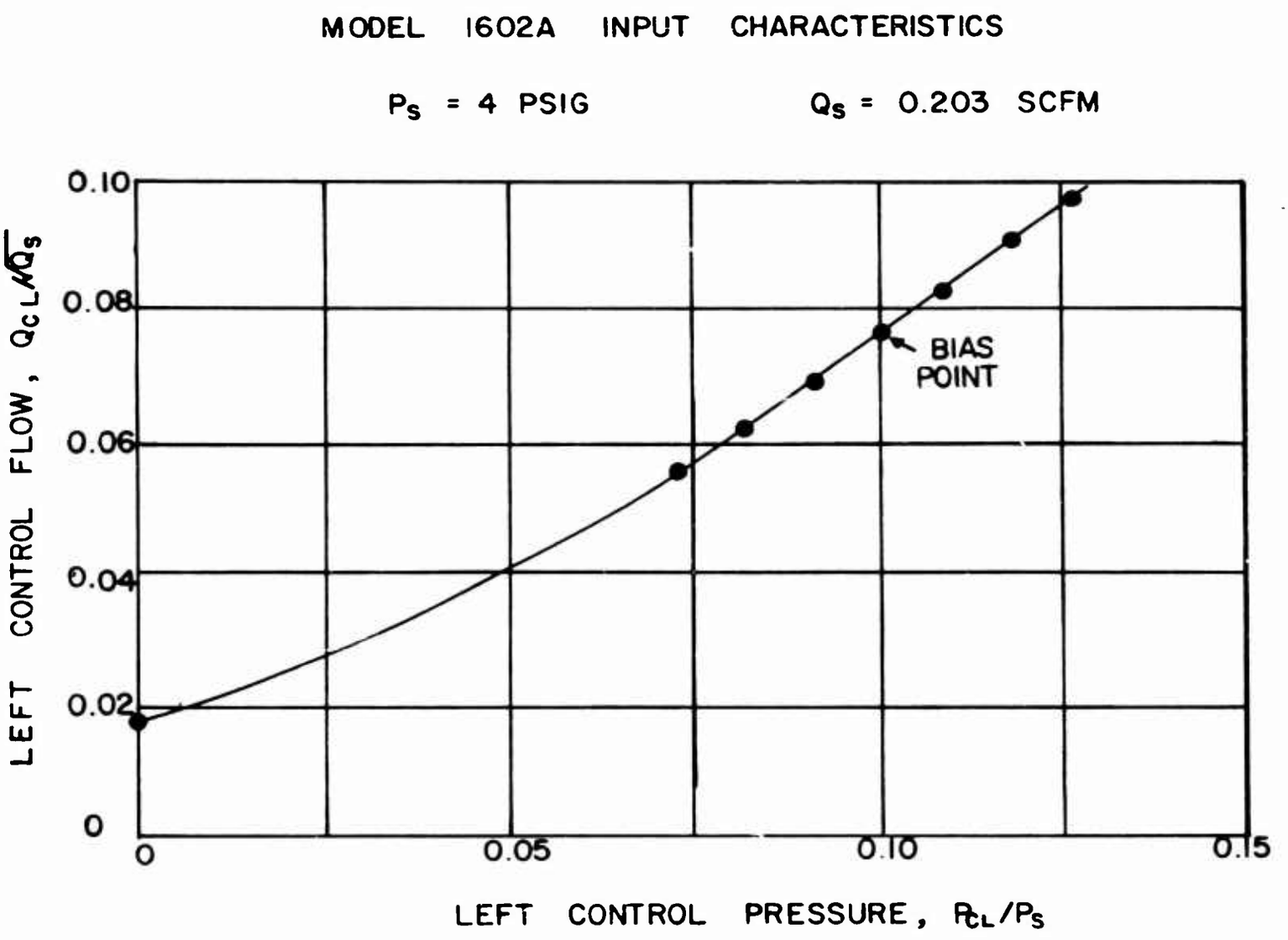

FIGURE 38 - NORMALIZED INPUT CHARACTERISTICS OF MODEL 1602A AT 4 PSI.

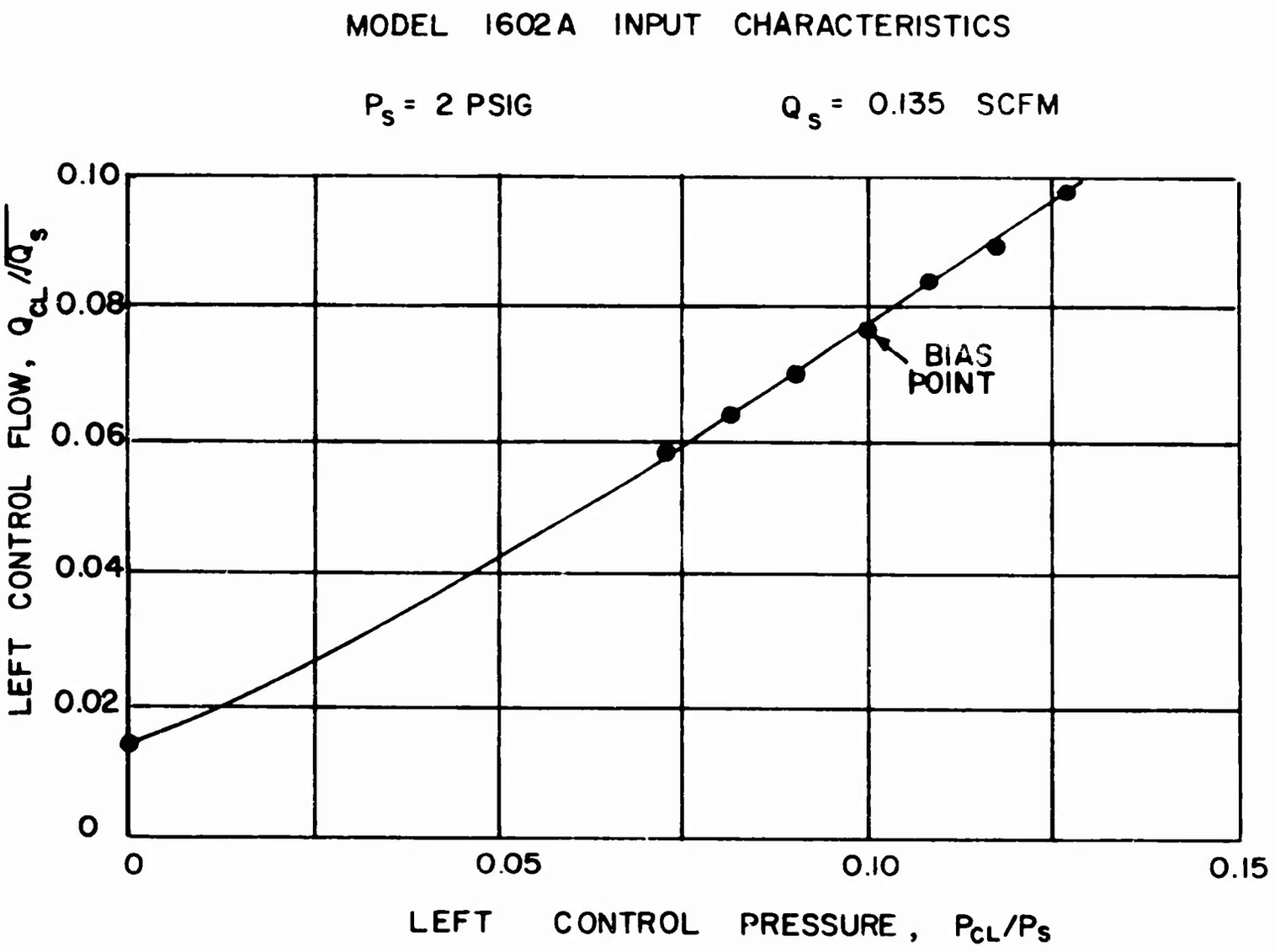

FIGURE 39 - NORMALIZED INPUT CHARACTERISTICS OF MODEL 1602A AT 2 PSI.

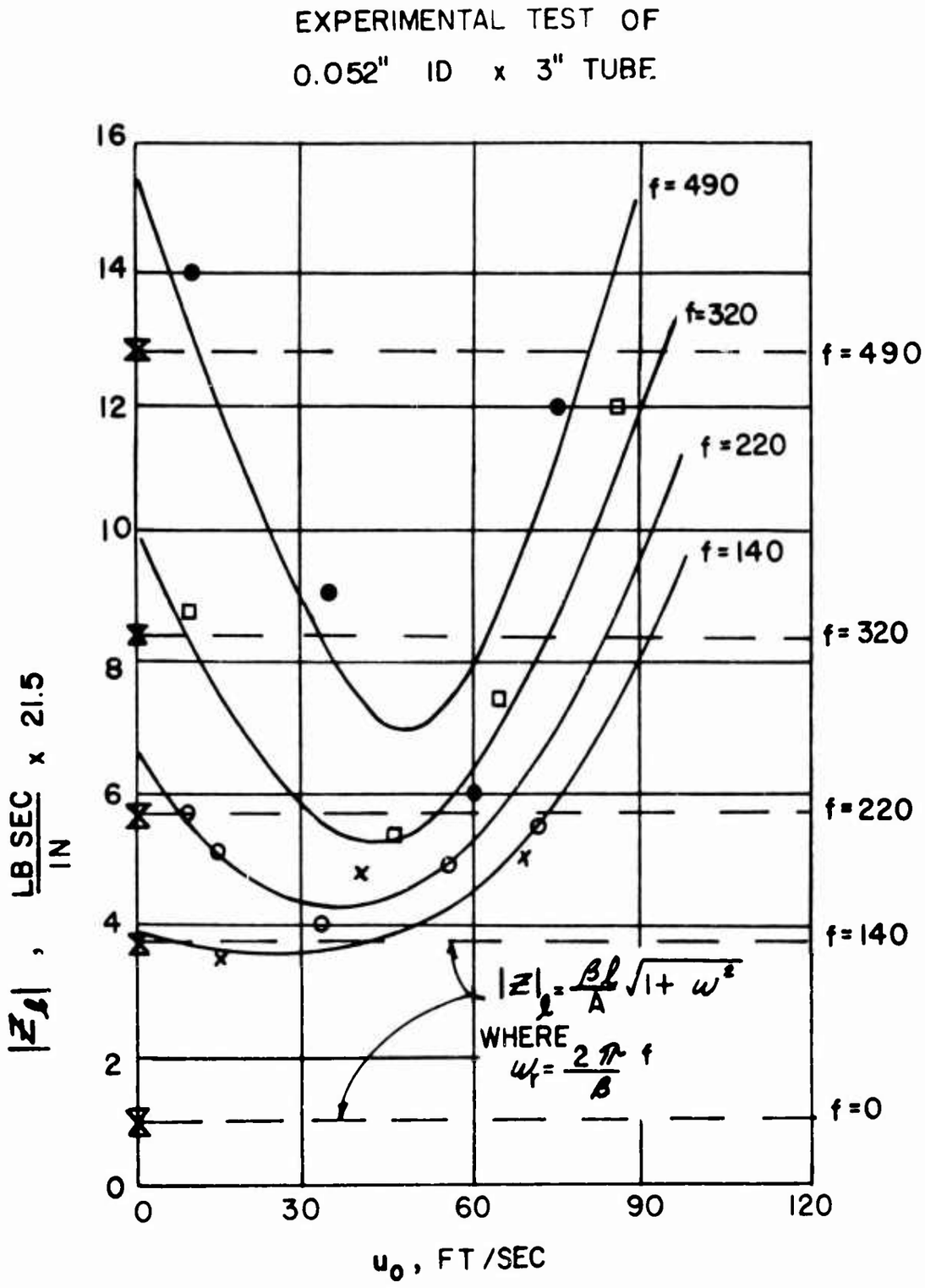

FIGURE 40 - EXPERIMENTAL TEST RESULTS OF TYPICAL IMPEDANCE ELEMENT.

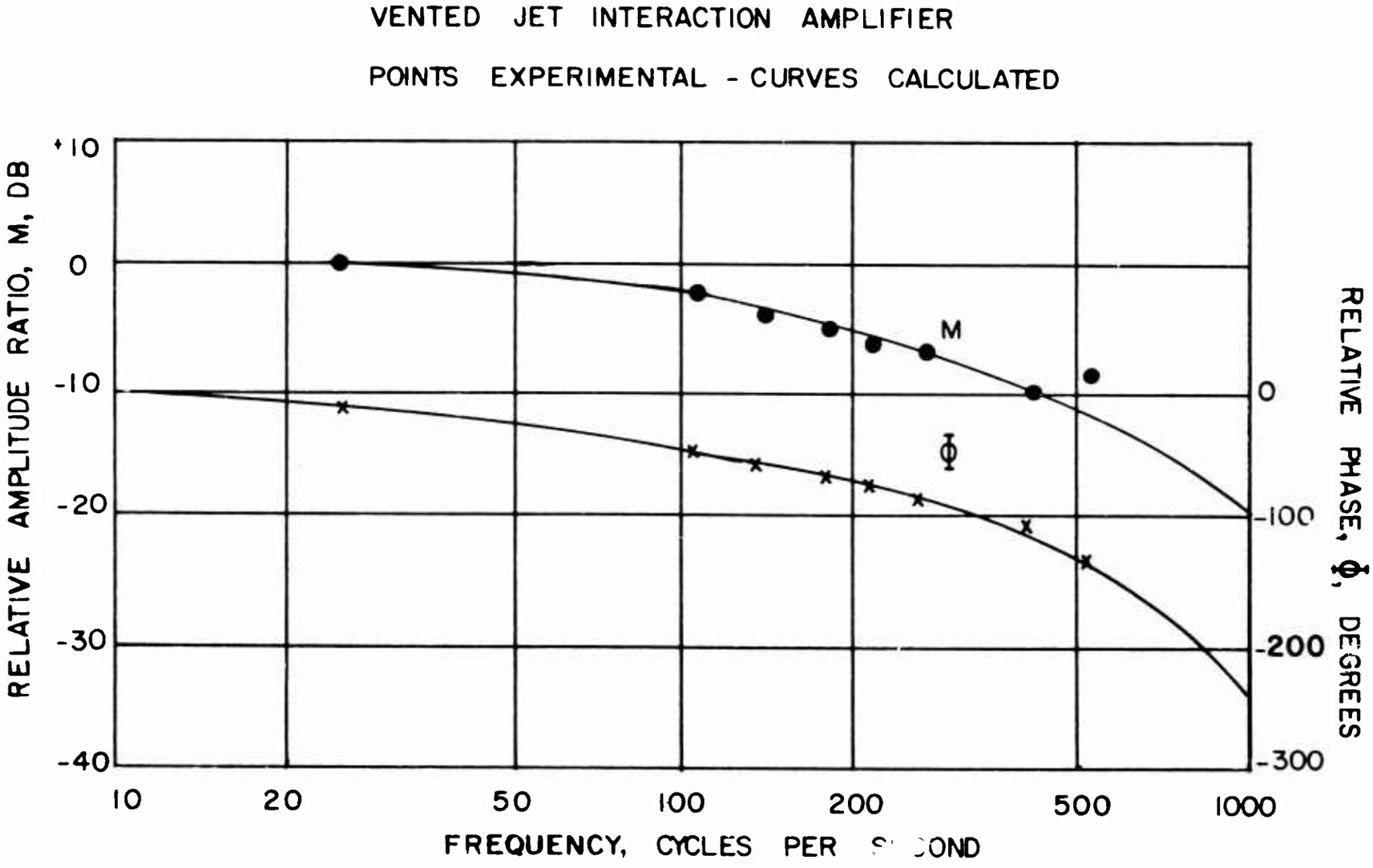

FIGURE 41 - CORRELATION OF FREQUENCY RESPONSE - VENTED JET INTERACTION AMPLIFIER.

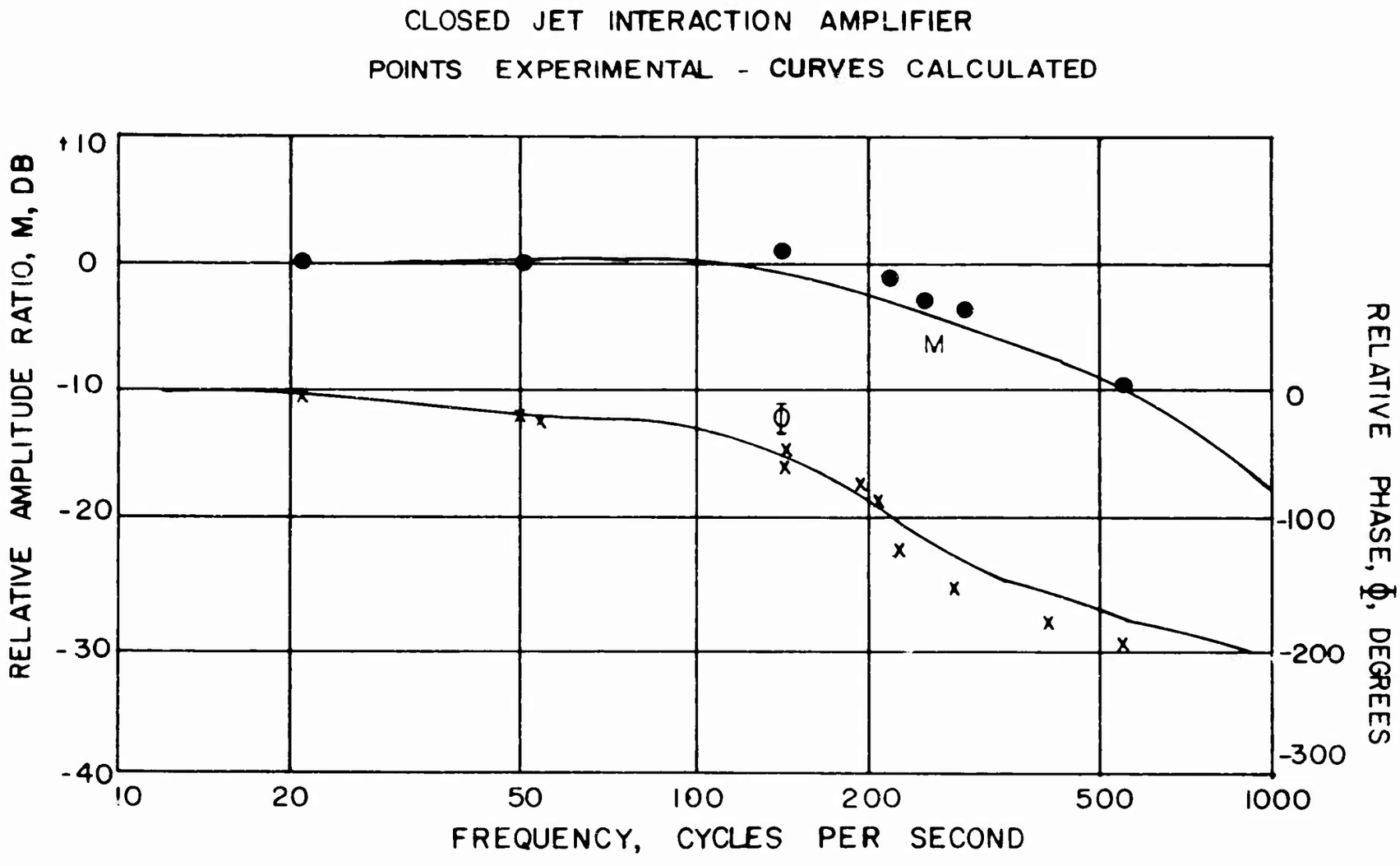

FIGURE 42 - CORRELATION OF FREQUENCY RESPONSE - CLOSED JET INTERACTION AMPLIFIER.

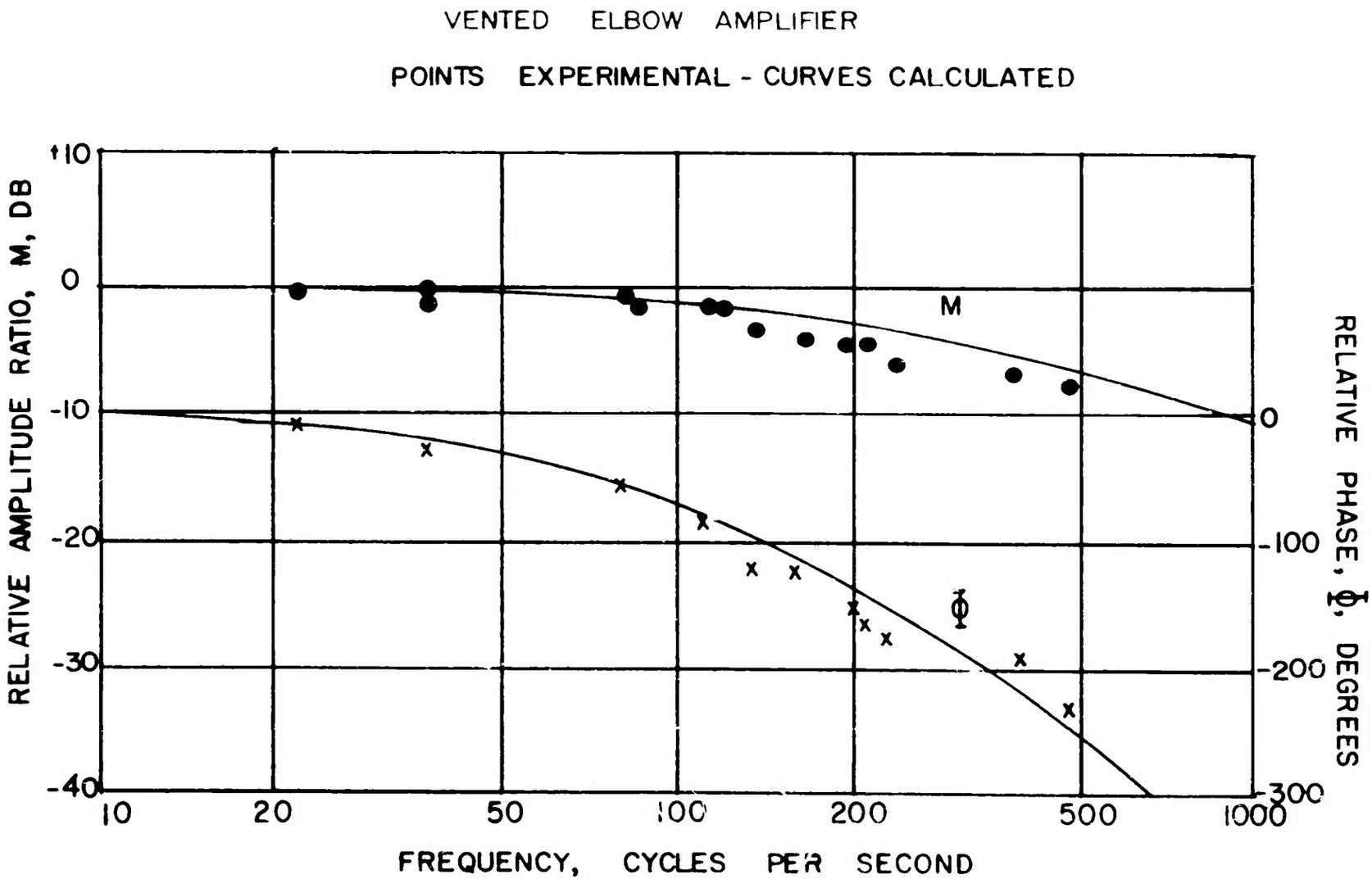

FIGURE 43 - CORRELATION OF FREQUENCY RESPONSE - VENTED ELBOW AMPLIFIER.

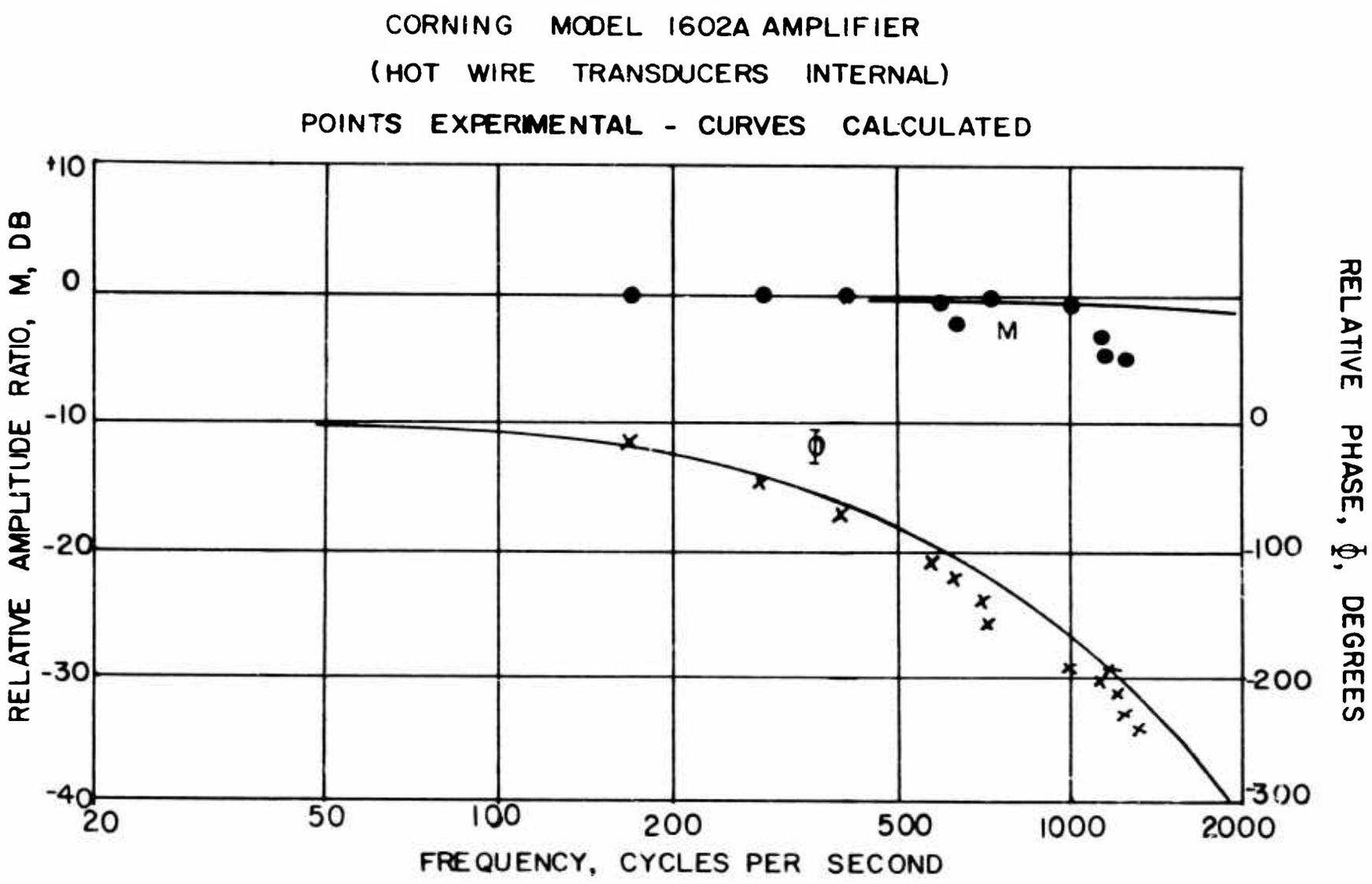

FIGURE 44 - CORRELATION OF FLOW RESPONSE AT HIGH FREQUENCIES.

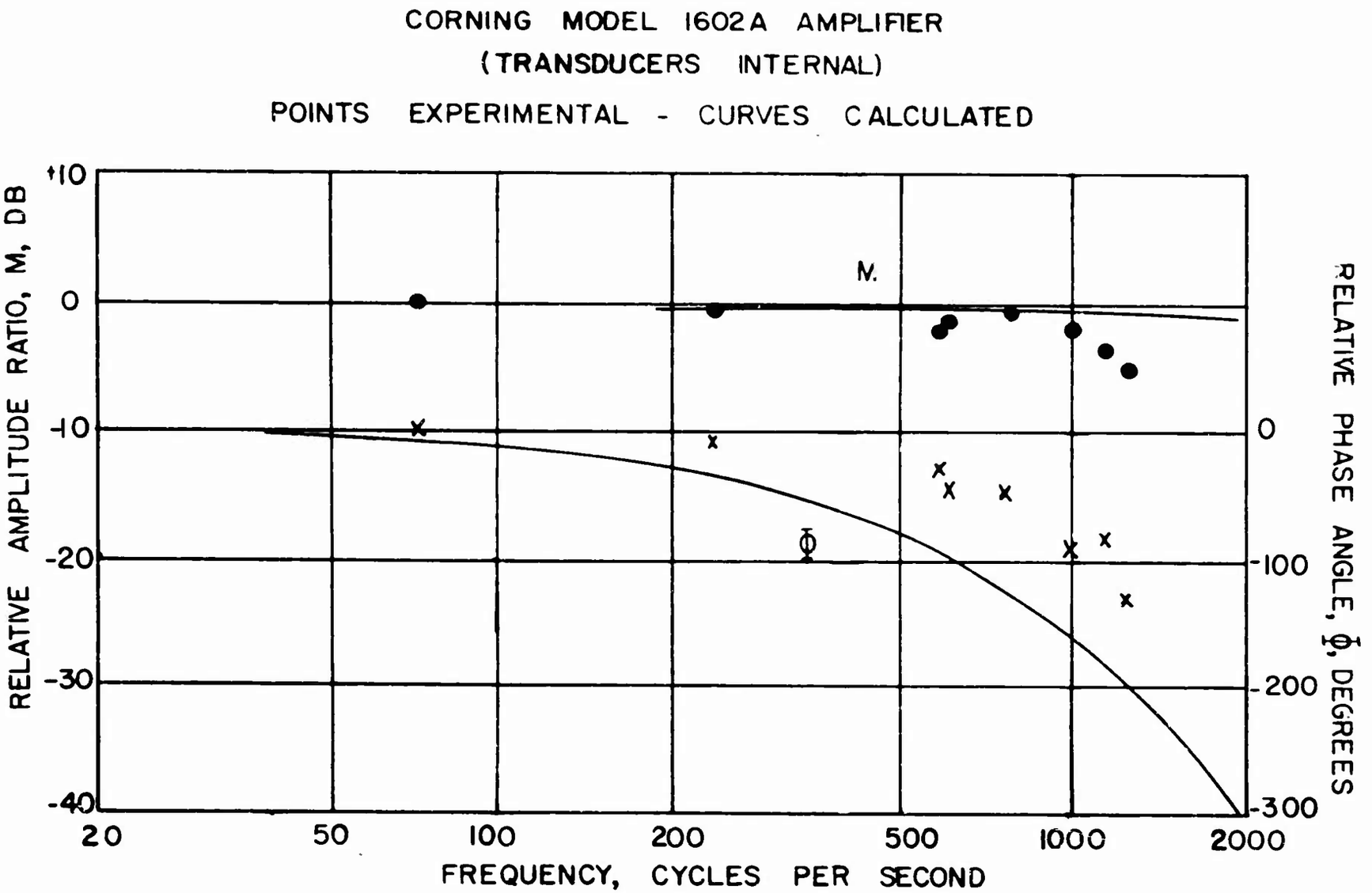

FIGURE 45 - CORRELATION OF PRESSURE RESPONSE AT HIGH FREQUENCIES.

BLANK PAGE

Unclassified

Security Classification

DOCUMENT CONTROL DATA - R&D

(Security classification of title, body of abstract and indexing annotation must be entered when the overall report is classified)

1 ORIGINATING ACTIVITY (Corporate author) Giannini Controls Corporation Astromechanics Research Division 179 Lancaster Ave., Malvern, Penna. 19355	2a REPORT SECURITY CLASSIFICATION Unclassified 2b GROUP

3 REPORT TITLE

DEVELOPMENT OF TECHNIQUES FOR THE STATIC AND DYNAMIC ANALYSIS OF FLUID STATE COMPONENTS AND SYSTEMS

4 DESCRIPTIVE NOTES (Type of report and inclusive dates)

Final Report 1 March 1965 through 31 October 1965

5 AUTHOR(S) (Last name, first name, initial)

Belsterling, Charles A.

6 REPORT DATE February 1966	7a TOTAL NO. OF PAGES 67	7b NO. OF REFS 6
8a CONTRACT OR GRANT NO. DA 44-177-AMC-284(T) b. PROJECT NO. c. Task 1P121401A14186 d.	9a ORIGINATOR'S REPORT NUMBER(S) USAAVLABS Technical Report 66-16 9b OTHER REPORT NO(S) (Any other numbers that may be assigned this report) ARD-FR 037	

10 AVAILABILITY/LIMITATION NOTICES

Distribution of this document is unlimited.

11 SUPPLEMENTARY NOTES	12 SPONSORING MILITARY ACTIVITY U. S. Army Aviation Materiel Laboratories Fort Eustis, Virginia

13 ABSTRACT

This report describes development of analytical techniques necessary for design of systems using fluidic components. It covers the analytical and experimental work on five separate tasks intended to extend the usefulness of previously conceived methods. The results lead to the following conclusions.

1) Valid equivalent circuits have been developed to describe the dynamic behavior of most fluid amplifiers.
2) These equivalent circuits are useful for frequencies from zero through 2000 cps.
3) The validity of certain methods previously developed for evaluating equivalent circuit elements has been confirmed.
4) Static characteristic curves of amplifier performance of the type developed under this program can be normalized, thereby minimizing the number of sets of curves necessary to describe the behavior of an amplifier.
5) The mathematical model derived for a simple impedance element is valid for low values of through-flow; additional work is needed to modify it for high through-flow values.

DD FORM 1 JAN 64 1473

Unclassified

Security Classification

14. KEY WORDS	LINK A		LINK B		LINK C	
	ROLE	WT	ROLE	WT	ROLE	WT
Fluidic Amplifiers Fluidic Systems Systems Analysis						

INSTRUCTIONS

1. ORIGINATING ACTIVITY: Enter the name and address of the contractor, subcontractor, grantee, Department of Defense activity or other organization *(corporate author)* issuing the report.

2*a*. REPORT SECURITY CLASSIFICATION: Enter the overall security classification of the report. Indicate whether "Restricted Data" is included. Marking is to be in accordance with appropriate security regulations.

2*b*. GROUP: Automatic downgrading is specified in DoD Directive 5200.10 and Armed Forces Industrial Manual. Enter the group number. Also, when applicable, show that optional markings have been used for Group 3 and Group 4 as authorized.

3. REPORT TITLE: Enter the complete report title in all capital letters. Titles in all cases should be unclassified. If a meaningful title cannot be selected without classification, show title classification in all capitals in parenthesis immediately following the title.

4. DESCRIPTIVE NOTES: If appropriate, enter the type of report, e.g., interim, progress, summary, annual, or final. Give the inclusive dates when a specific reporting period is covered.

5. AUTHOR(S): Enter the name(s) of author(s) as shown on or in the report. Enter last name, first name, middle initial. If military, show rank and branch of service. The name of the principal author is an absolute minimum requirement.

6. REPORT DATE: Enter the date of the report as day, month, year; or month, year. If more than one date appears on the report, use date of publication.

7*a*. TOTAL NUMBER OF PAGES: The total page count should follow normal pagination procedures, i.e., enter the number of pages containing information.

7*b*. NUMBER OF REFERENCES: Enter the total number of references cited in the report.

8*a*. CONTRACT OR GRANT NUMBER: If appropriate, enter the applicable number of the contract or grant under which the report was written.

8*b*, 8*c*, & 8*d*. PROJECT NUMBER: Enter the appropriate military department identification, such as project number, subproject number, system numbers, task number, etc.

9*a*. ORIGINATOR'S REPORT NUMBER(S): Enter the official report number by which the document will be identified and controlled by the originating activity. This number must be unique to this report.

9*b*. OTHER REPORT NUMBER(S): If the report has been assigned any other report numbers *(either by the originator or by the sponsor)*, also enter this number(s).

10. AVAILABILITY/LIMITATION NOTICES: Enter any limitations on further dissemination of the report, other than those imposed by security classification, using standard statements such as:

(1) "Qualified requesters may obtain copies of this report from DDC."

(2) "Foreign announcement and dissemination of this report by DDC is not authorized."

(3) "U. S. Government agencies may obtain copies of this report directly from DDC. Other qualified DDC users shall request through _____."

(4) "U. S. military agencies may obtain copies of this report directly from DDC. Other qualified users shall request through _____."

(5) "All distribution of this report is controlled. Qualified DDC users shall request through _____."

If the report has been furnished to the Office of Technical Services, Department of Commerce, for sale to the public, indicate this fact and enter the price, if known.

11. SUPPLEMENTARY NOTES: Use for additional explanatory notes.

12. SPONSORING MILITARY ACTIVITY: Enter the name of the departmental project office or laboratory sponsoring *(paying for)* the research and development. Include address.

13. ABSTRACT: Enter an abstract giving a brief and factual summary of the document indicative of the report, even though it may also appear elsewhere in the body of the technical report. If additional space is required, a continuation sheet shall be attached.

It is highly desirable that the abstract of classified reports be unclassified. Each paragraph of the abstract shall end with an indication of the military security classification of the information in the paragraph, represented as *(TS)*, *(S)*, *(C)*, *or (U)*.

There is no limitation on the length of the abstract. However, the suggested length is from 150 to 225 words.

14. KEY WORDS: Key words are technically meaningful terms or short phrases that characterize a report and may be used as index entries for cataloging the report. Key words must be selected so that no security classification is required. Identifiers, such as equipment model designation, trade name, military project code name, geographic location, may be used as key words but will be followed by an indication of technical context. The assignment of links, rules, and weights is optional.

1227-66